UNIVERSITY OF CALIFORNIA
DIVISION OF ELECTRICAL ENGINEERING
BERKELEY, CALIFORNIA

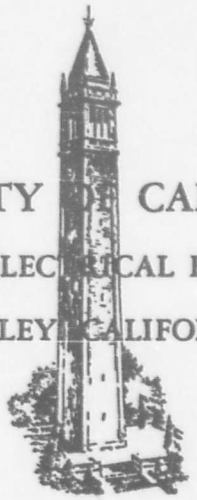

ELECTRONICS RESEARCH LABORATORY

LINEAR ARRAYS WITH ARBITRARILY DISTRIBUTED ELEMENTS

by
H. Unz

Institute of Engineering Research
Series No. 60, Issue No. 168
November 2, 1956

DIVISION OF ELECTRICAL ENGINEERING

ELECTRONICS RESEARCH LABORATORY

SERIES NO. 60
ISSUE NO. 168

ANTENNA GROUP

LINEAR ARRAYS WITH ARBITRARILY DISTRIBUTED ELEMENTS

by

H. Unz

Report No. 56 on
Office of Naval Research
Contract N7onr-29529

November 2, 1956

CONTENTS

ABSTRACT

A linear array with general arbitrarily distributed elements is discussed. A matrix relation is found between the elements of the array and its far zone pattern. The radiated power is shown to consist of distinct modes; the magnitude of each is related directly to the elements.

The total radiated power is calculated for basic, broadside and end-fire arrays, in terms of the interaction coefficients. The lower bound of the stored energy and the Q factor of the array are found. A figure of merit for the array is defined. A method of analyzing a given array from amplitude measurements of the pattern is given.

Two examples are given for linear arrays which produce a prescribed pattern. Comparison between an array with equi-spaced elements and an array with arbitrarily distributed elements shows that the latter requires fewer elements and gives better performance.

INTRODUCTION

From the early days of radio communications, the importance of directive antennas was realized. The principles of wave interference, on which systems of directive radio are based, have been known probably for several centuries. However, the first thorough treatment of this subject was conducted by Fresnel and Huygens, who established the wave theory of light in the early part of the nineteenth century.

In 1937 Wolff[1] published his important method of obtaining any arbitrary far zone circular symmetric pattern from radiators with equidistant distribution along an array axis. His theory was based upon comparison of the far zone field of a pair of radiators to a term of Fourier series expansion of the prescribed pattern.

In 1943 Schelkunoff[2], in his remarkable article, utilized the correspondence between nulls of the pattern of a linear array with equidistant elements and the roots of a complex polynomial in the complex plane. He derived different types of pattern variations by choosing the zeros and thereby obtaining an improvement in the side lobe level over that of the uniform case.

In 1946 Dolph[3] devised his important method of synthesizing an optimum pattern for a broadside array. An optimum pattern is defined as a pattern for which the beam width is a minimum for a given side lobe level, or on the other hand, the side lobe level is minimum for a given beam width. The optimum pattern is obtained from Tchebycheff polynomials, and has equal side lobes.

In 1948 Woodward and Lawson[4] used an infinite number of plane waves to show that a super-gain, as well as a specified radiation pattern, may be obtained from an aperture of a given size. They gave the stored energy of the system as a line integral in the complex θ-plane. In practice, no super-gain is possible for two reasons: (a) The currents in the conducting elements of the source become very large with an increase in the copper-loss. (b) The stored energy of the super-gain array becomes very large. Therefore the shape of the radiation pattern and the impedance of the aerial would be extremely sensitive to small changes of frequency, and manufacturing tolerances could become prohibitive.

The complete analysis of the problem in terms of spherical modes was

given by Chu[5]. He considered an arbitrary source confined by a sphere and calculated the maximum gain - Q ratio obtainable from a system of a given size. Only a finite number of spherical modes will radiate from a source of a given size and the remainder of them will act mainly as stored energy around the source.

After most of the material in this report had been written, a French thesis by Arsac[6] was brought to the attention of the author. Arsac discussed antennas for radio astronomy where the ratios of the spacings between the elements are integers. He also discussed there some ideas regarding the mode theory.

1. Relations between Pattern and Sources

It may be shown[7] that the far zone pattern of a linear array with arbitrarily distributed similar elements is given by:

$$F(\theta,\varphi)=\lambda\ (\theta,\varphi)\ \sum_{\ell=0}^{L}\ A_\ell e^{ikx_\ell\cos\theta} \tag{1}$$

where: $F(\theta,\varphi)$ = Far zone pattern of array

$\lambda(\theta,\varphi)$ = far zone pattern of a single element

A_ℓ = current (complex) in magnitude and phase of element ℓ.

x_ℓ = position of element ℓ on the axis of the array.

$k = \frac{2\pi}{\lambda} = \frac{\omega}{c}$

θ,φ = variable angles (see Fig. 1)

(1) may be rewritten as:

$$F(\theta) = \frac{F(\theta,\varphi)}{\lambda(\theta,\varphi)} = \sum_{\ell=0}^{L}\ A_\ell e^{ikx_\ell\cos\theta} \tag{2}$$

where $F(\theta)$ is the radiation pattern of a linear array with arbitrarily distributed isotropic radiators.

Let us consider also the complementary angle ϕ (Fig. 1) such that:

$$\phi + \theta = \frac{\pi}{2} \qquad\qquad \cos\theta = \sin\phi \tag{3}$$

Using (3) we can write (2) as:

$$F(\phi) = \sum_{\ell=0}^{L}\ A_\ell e^{ikx_\ell\sin\phi} \tag{4a}$$

$$F(\theta) = \sum_{\ell=0}^{L}\ A_\ell\ e^{ikx_\ell\cos\theta} \tag{4b}$$

We have the following Jacobi expansions[8]:

$$e^{iz\sin\phi} = \sum_{n=-\infty}^{+\infty}\ e^{in\phi}J_n(z) \tag{5a}$$

$$e^{iz\cos\theta} = \sum_{n=-\infty}^{+\infty}\ i^n e^{in\theta}J_n(z) \tag{5b}$$

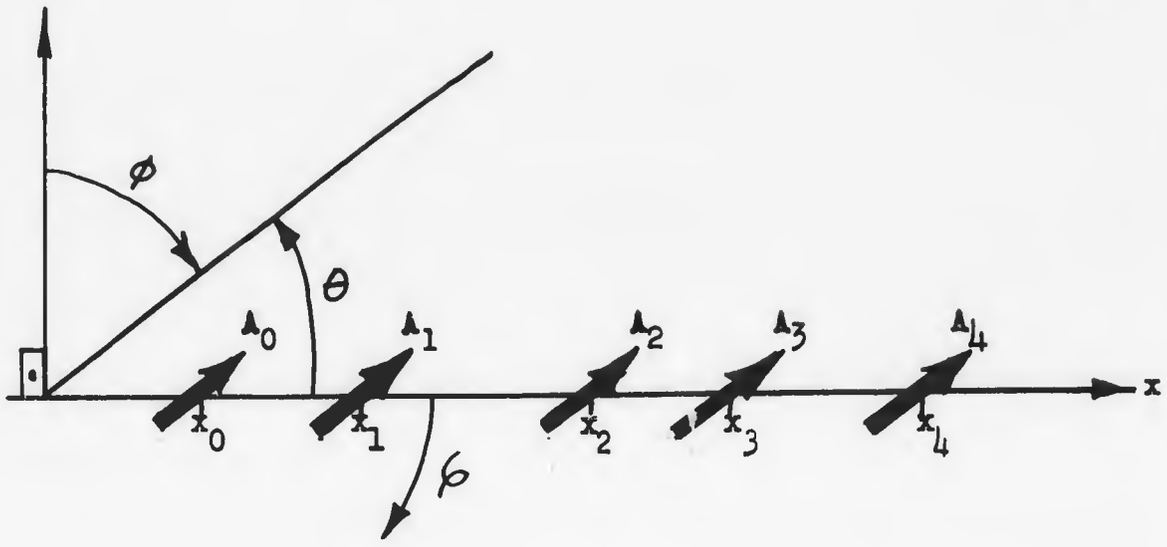

Fig. 1. Linear Array

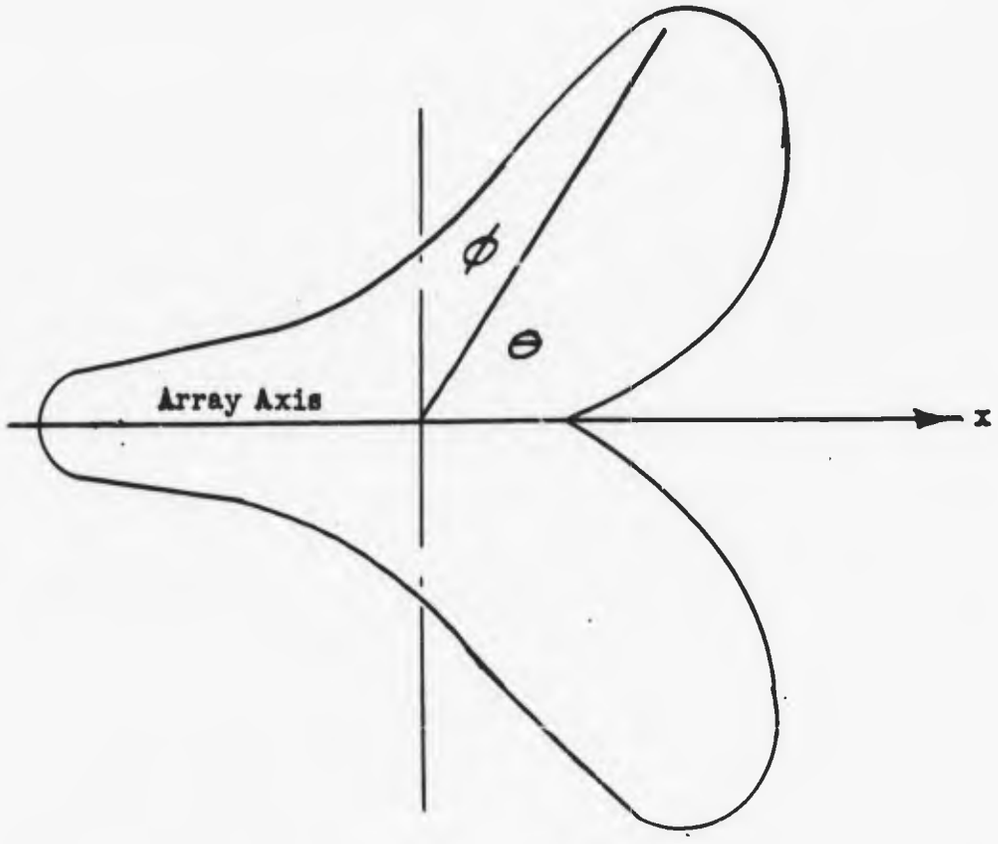

Fig. 2. Pattern Symmetry

Taking in (5a) $z=kx_\ell$ and substituting in (4a) we get:

$$F(\phi) = \sum_{\ell=0}^{L} A_\ell \sum_{n=-\infty}^{+\infty} e^{in\phi} J_n(kx_\ell) \tag{6}$$

Since $F(\phi)$ is a periodic function with respect to ϕ, it can be expanded in a complex Fourier series:

$$F(\phi) = \sum_{n=-\infty}^{+\infty} f_n e^{in\phi} \tag{7a}$$

$$f_n = \frac{1}{2\pi} \int_{-\pi}^{\pi} F(\phi) e^{-in\phi} d\phi \tag{7b}$$

comparing (7a) with (6) we see the relation:

$$f_n = \sum_{\ell=0}^{L} A_\ell J_n(kx_\ell) \tag{8}$$

(8) gives a direct relation between the currents in the elements of the array, their distribution along the axis of the array, and the coefficients of the Fourier expansion of the radiation pattern.

From the theory of Bessel functions it is known[8] that:

$$J_{-n}(z) = (-)^n J_n(z) \tag{9}$$

From (8) and (9) we get that:

$$f_{-n} = (-)^n f_n \tag{10}$$

From Fig. 2 we see that the conditions for $F(\phi)$, $F(\theta)$ to be symmetric with respect to the array axis x are:

$F(\theta)=F(-\theta)$ $\quad F(\pi - \theta) = F(\pi+\theta)$ $\quad$ symmetric like cos θ (11a)

$F(\phi)=F(\pi- \phi)$ $\quad F(\phi-\pi)=F(-\phi)$ $\quad$ symmetric like sin ϕ (11b)

It may be shown easily that (10) is the necessary and sufficient condition

in (7a) for (11b) to exist.

Since (8) must hold for every n, it may be written in a matrix form:

$$\begin{bmatrix} f_o \\ f_1 \\ f_2 \\ \vdots \\ f_n \\ \vdots \end{bmatrix} = \begin{bmatrix} J_o(kx_o) & J_o(kx_1) & \cdots & J_o(kx_L) \\ J_1(kx_o) & J_1(kx_1) & \cdots & J_1(kx_L) \\ J_2(kx_o) & J_2(kx_1) & \cdots & J_2(kx_L) \\ \vdots & \vdots & & \vdots \\ J_n(kx_o) & J_n(kx_1) & & J_n(kx_L) \\ \vdots & \vdots & & \vdots \end{bmatrix} \cdot \begin{bmatrix} A_o \\ A_1 \\ A_2 \\ \vdots \\ A_L \end{bmatrix} \tag{12a}$$

or in short:

$$f] = [J] \cdot A] \tag{12b}$$

The matrix $[J]$ has $L+1$ columns but infinite number of rows because, from a finite number of radiators, we can get as many Fourier coefficients as desired. However, from a certain row on, the coefficients become negligibly small in magnitude.

In case we want to get a prescribed pattern from $L+1$ radiators, we have to find the inverse matrix

$$A] = [J]^{-1} \cdot f] \tag{13}$$

but then we can use only the first $L+1$ coefficients f_n of the Fourier series in order for $[J]$ to become a square matrix.

If we use Θ as the variable angle, by substituting (5b) into (4b), and using the above methods we get

$$F(\Theta) = \sum_{n=-\infty}^{+\infty} g_n e^{in\Theta} \tag{14a}$$

$$i^{-n} g_n = \sum_{l=0}^{L} A_l J_n(kx_l) \tag{14b}$$

Another useful relation is based on the following spherical Bessel function identity given by Bauer[8]:

$$e^{iz\cos\Theta} = \sum_{n=0}^{\infty} (2n+1)\, i^n\, j_n(z)\, P_n(\cos\Theta) \tag{15}$$

where

$$j_n(z) = \sqrt{\frac{\pi}{2z}}\ J_{n+1/2}\ (z) = \text{spherical Bessel function}^9$$

$P_n(\cos\theta)$ = Legendre polynomials.

Substituting (15) in (4b) with $z=kx_\ell$ and rearranging we get:

$$F(\theta) = \sum_{n=0}^{\infty} (2n+1)\, i^n P_n(\cos\theta) \sum_{\ell=0}^{L} A_\ell j_n(kx_\ell) \tag{16}$$

and since $F(\theta)$ has the same symmetry relations as $\cos\theta$, as is seen from (11a), it may be expanded by Legendre polynomials with $\cos\theta$ as the variable:

$$F(\theta) = \sum_{n=0}^{\infty} (2n+1) d_n P_n(\cos\theta) \tag{17a}$$

$$d_n = \frac{1}{2}\int_0^{\pi} F(\theta) P_n(\cos\theta)\sin\theta d\theta \tag{17b}$$

(17) is based on the orthogonality properties of Legendre polynomials[9]:

$$\int_0^{\pi} P_n(\cos\theta) P_m(\cos\theta)\sin\theta d\theta = \frac{2}{2n+1}\,\delta_{m,n} \tag{18}$$

where:

$$\delta_{m,n} = \begin{cases} 1 & m=n \\ 0 & m\neq n \end{cases}$$

comparing (16) with (17a) we get:

$$i^{-n} d_n = \sum_{\ell=0}^{L} A_\ell j_n(kx_\ell) \tag{19}$$

It must be noted that expansion (17a) obeys automatically the symmetries required by (11a) since $\cos\theta$ has the same symmetries.

(15) is a particular case of the more general care given by Gegenbauer[8]

$$e^{iz\cos\theta} = 2^\nu \Gamma(\nu) \sum_{n=0}^{\infty} (\nu+n) i^n \frac{J_{\nu+n}(z)}{z^\nu} C_n^\nu(\cos\theta) \tag{20}$$

where: $C_n^\nu(\cos\theta)$ = Gegenbauer polynomials defined[10] by:

$$\frac{1}{(1-2z\cos\theta + z^2)^{\nu}} = \sum_{n=0}^{\infty} C_n^{\nu}(\cos\theta) z^n \tag{21a}$$

$$C_n^{\nu}(\cos\theta) = \sum_{\substack{p,q=0 \\ p+q=n}}^{n} \frac{\Gamma(\nu+p)\,\Gamma(\nu+q)}{\Gamma^2(\nu)\,p!\,q!} \cos(p-q)\theta \tag{21b}$$

It must be noted that

$$C_n^{1/2}(\cos\theta) = P_n(\cos\theta) \tag{22}$$

Let us define the general spherical Bessel function in the form:

$$j_n^{\nu}(z) = 2^{\nu-1}\Gamma(\nu)\,\frac{J_{\nu+n}(z)}{z^{\nu}} \quad \text{for} \quad \nu > 0 \tag{23}$$

It must be noted that, since" $\Gamma(\frac{1}{2}) = \sqrt{\pi}$:

$$j_n^{1/2}(z) = j_n(z) \tag{24}$$

Using the definition in (23), we can rewrite (20) in the form:

$$e^{iz\cos\theta} = 2\sum_{n=0}^{\infty} (\nu+n) i^n\, j_n^{\nu}(z) C_n^{\nu}(\cos\theta) \tag{25}$$

which is identical with (15) when $\nu=1/2$ due to (22) and (24). Gegenbauer polynomials have the orthogonality properties[10]:

$$\int_0^{\pi} \sin^{2\nu}\theta\; C_n^{\nu}(\cos\theta) C_m^{\nu}(\cos\theta)\, d\theta = \frac{\pi\,\Gamma(2\nu+n)}{2^{2\nu-1}(\nu+n)n!\Gamma^2(\nu)}\,\delta_{m,n} \tag{26}$$

Using (26), $F(\theta)$ may be expanded in Gegenbauer polynomials:

$$F(\theta) = 2\sum_{n=0}^{\infty} (\nu+n)\, h_n^{\nu} C_n^{\nu}(\cos\theta) \tag{27a}$$

$$h_n^{\nu} = \frac{\Gamma^2(\nu)\; n!}{\pi\,\Gamma(2\nu+n)}\; 2^{2\nu-2} \int_0^{\pi} F(\theta) C_n^{\nu}(\cos\theta) \sin^{2\nu}\theta d\theta \tag{27b}$$

Comparing (27) to (17) we see from (22) that:

$$h_n^{1/2} = d_n \tag{28}$$

Substituting (25) in (4b) and comparing to (27a) we get:

$$i^{-n}h_n^{\nu} = \sum_{\ell=0}^{L} A_\ell j_n^{\nu}(kx_\ell) \tag{29}$$

(29) is identical with (19) for $\nu = 1/2$ due to (24) and (28). Since it can be shown[10] that

$$\lim_{\nu\to 0} \Gamma(\nu) C_n^{\nu}(\cos\theta) = \frac{2}{n}\cos n\theta \tag{30a}$$

$$C_0^{0}(\cos\theta) = 1 \qquad \lim_{\nu\to 0} \nu\Gamma(\nu) = 1 \tag{30b}$$

Substituting (23) into (25) and taking $\nu\to 0$, we get, due to (30),

$$e^{iz\cos\theta} = J_0(z) + 2\sum_{n=1}^{\infty} i^n J_n(z)\cos n\theta \tag{31}$$

However, (31) is identical with (5b) and, (5b) is only a degenerate case of (25) for $\nu\to 0$. Also, (14b) is a degenerate case of (29) for $\nu\to 0$.

Since A_ℓ are complex numbers in general, all the coefficients f_n, g_n, d_n, h_n^{ν} are complex numbers in general.

Let us summarize the above in Table I. Numbers in parenthesis refer to formulaes.

TABLE I

Pattern	variable ϕ	variable θ		
	$F(\phi)$	$F(\theta)$		
function of expansion	(7a) $e^{in\phi}$	$\nu\neq 0$ (27a) $C_n^{\nu}(\cos\theta)$	$\nu=1/2$ (17a) $P_n(\cos\theta)$	deg. $\nu\to 0$ (14a) $e^{in\theta}$
coefficient of expansion	(7b) f_n	(27b) h_n^{ν}	(17b) d_n	(7b) g_n
function of radiator position	(8) $J_n(kx_\ell)$	(29) $j_n^{\nu}(kx_\ell)$	(19) $j_n(kx_\ell)$	(14b) $J_n(kx_\ell)$

2. The Radiated Modes

In this section we shall show that the radiated power from a linear array consists of distinct spherical modes. It may be shown that the far zone electric field from a linear array is given by:

$$E = -\frac{i\omega\mu}{4\pi}\ \frac{e^{-ikR}}{R}\ F(\theta,\varphi) \tag{32}$$

where (θ,φ) are the spherical coordinates. The total radiated power is given by:

$$P = \frac{1}{\eta}\int_0^{2\pi} d\varphi \int_0^{\pi} \sin\theta d\theta\ R^2\ |E|^2 \tag{33}$$

where $\eta = \sqrt{\frac{\mu}{\epsilon}}$ = radiation resistance.
Substituting (32) into (33) and rearranging we get:

$$P = \frac{\omega^2\mu^2}{4\pi\eta}\ \frac{1}{4\pi}\int_0^{2\pi} d\varphi \int_0^{\pi} \sin\theta d\theta\ |F(\theta,\varphi)|^2 \tag{34}$$

we shall consider 3 cases:

Case I: Basic Array (Fig. 3a). Ann array with isotropic radiators as the elements. Although the array with isotropic radiators as the elements cannot be achieved physically, it is a useful mathematical tool. In this case we have to put in (1):

$$\lambda(\theta,\psi) = 1;\ F(\theta,\psi) = F(\theta) \tag{35}$$

where $F(\theta)$ is defined by (2). Substituting in (34) we get:

$$P_B = \frac{\omega^2\mu^2}{4\pi\eta}\ \frac{1}{2}\int_0^{\pi} |F(\theta)|^2\ \sin\theta d\theta \tag{36}$$

Using the expansion of $F(\theta)$ in (17a) we get:

$$|F(\theta)|^2 = F(\theta)\cdot F(\theta)^* = \sum_{n=0}^{\infty}\sum_{m=0}^{\infty}(2n+1)(2m+1)d_n d_m^*\ P_n(\cos\theta)\ P_m(\cos\theta) \tag{37}$$

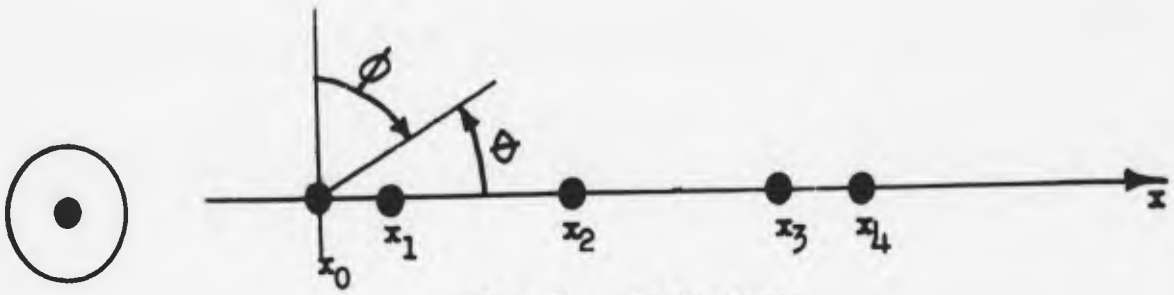

Fig. 3a. Basic Array

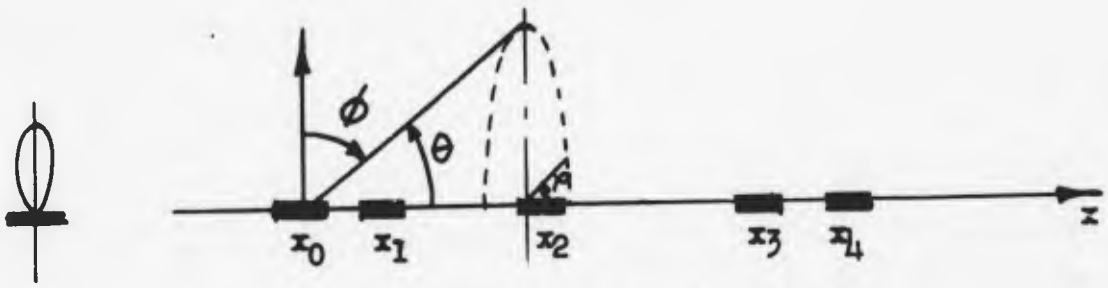

Fig. 3b. Broadside Array

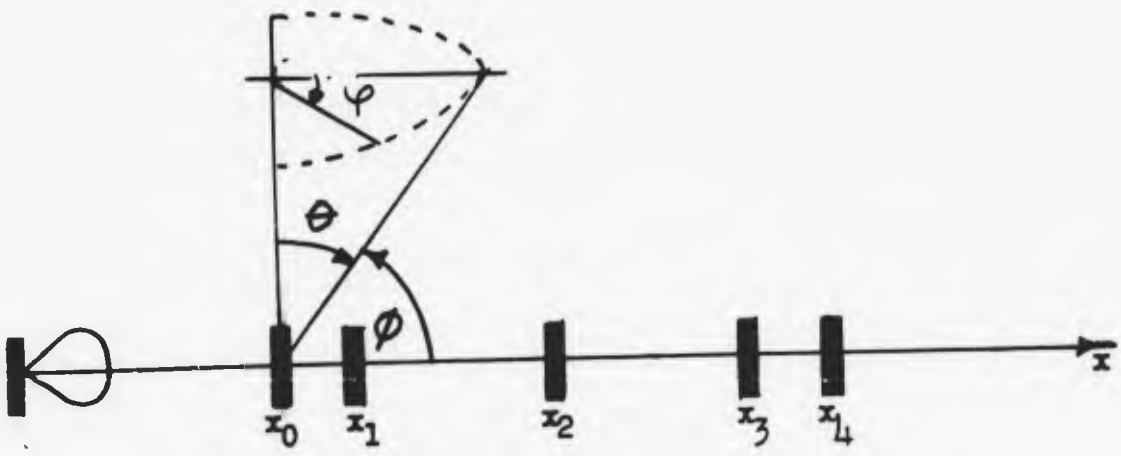

Fig. 3c. End-Fire Array

Substituting (37) in (36) and using the orthogonality property in (18) we get:

$$P = \frac{\omega^2\mu^2}{4\pi\eta} \sum_{n=0}^{\infty} (2n+1) |d_n|^2 \tag{38}$$

where d_n is given by (19). (38) shows that the total radiated power consists of an infinite number of modes.

In case of only one isotropic radiator we will have:

$$|d_n|^2 = |A_o|^2 j_n^2(kx_o) \tag{39}$$

From Appendix A equation (A-8):

$$\sum_{n=0}^{\infty} (2n+1) j_n^2(z) = 1 \tag{40}$$

Substituting (39) in (38) and using (40) we see that the total radiated power from a single element of the basic array is constant and is independent of the position of the origin. This could have been foreseen by physical argument. However, the distribution of the total radiated power among the different modes is dependent on the position of the chosen origin. The further the origin from the radiator, the more higher order modes are radiated, as may be seen from spherical Bessel function curves. The total power of a certain mode depends on the distribution of the radiators along the axis of the array.

Case II: Broadside Array (Fig. 3b). An array with radiators of circular pattern $\lambda(\theta)$, the axis of which is parallel to the axis of the array. In this case:

$$F(\theta,\varphi) = \lambda(\theta) F(\theta) \tag{41}$$

Substituting in (34) we get:

$$P_S = \frac{\omega^2\mu^2}{4\pi\eta} \frac{1}{2} \int_0^{\pi} |F(\theta)|^2 \lambda^2(\theta) \sin\theta d\theta \tag{42}$$

Let us first take the simplest case of dipoles where

$$\lambda(\theta) = \sin\theta \tag{43}$$

Using the expansion in (27a) for $\nu=\frac{3}{2}$ we get:

$$|F(\theta)|^2 = \sum_{m=0}^{\infty} \sum_{n=0}^{\infty} (2m+3)(2n+3)\, h_m^{3/2} h_n^{3/2*} C_m^{3/2}(\cos\theta)\, C_n^{3/2}(\cos\theta) \qquad (44)$$

Substituting (44) and (43) into (42) and using the orthogonality properties in (26) we get:

$$P_S^{(d)} = \frac{\omega^2\mu^2}{4\pi\eta} \frac{\pi}{2^2\Gamma^2(\frac{3}{2})} \sum_{n=0}^{\infty} (2n+3) \frac{\Gamma(n+3)}{n!} \left| h_n^{3/2} \right|^2 \qquad (45)$$

but since

$$\Gamma(\tfrac{3}{2}) = \tfrac{1}{2}\Gamma(\tfrac{1}{2}) = \tfrac{1}{2}\sqrt{\pi} \qquad \Gamma(n+1) = n! \qquad (46)$$

(45) becomes:

$$P_S^{(d)} = \frac{\omega^2\mu^2}{4\pi\eta} \sum_{n=0}^{\infty} (n+1)(n+2)(2n+3) \left| h_n^{3/2} \right|^2 \qquad (47)$$

where $h_n^{3/2}$ is given by (29). (47) shows that in the case of broadside arrays with dipole elements, the radiated power consists of infinite number of modes.

By using (29) and the identity in (A-11) it may be shown easily in (47) that the total power radiated from one dipole is constant and independent of the position of the origin.

For the more general case of general circular pattern for each element, let us expand:

$$\lambda^2(\theta) = \sum_{q=2}^{\infty} \alpha_q \sin^q\theta \qquad 0 \leqslant \theta \leqslant \pi \qquad (48)$$

(48) is a general expansion for $\lambda^2(\theta)$ due to the circular symmetry of the pattern around the element. Substituting (48) in (42) we get:

$$P_S = \frac{\omega^2\mu^2}{4\pi\eta} \sum_{q=2}^{\infty} \alpha_q \frac{1}{2} \int_0^{\pi} |F(\theta)|^2 \sin^{q+1}\theta d\theta \qquad (49)$$

Taking expansion (27a) and using the orthogonality properties (26) we get, similarily to the above:

$$\int_0^{\pi} |F(\theta)|^2 \sin^{2\nu}\theta d\theta = 4 \frac{\pi}{2^{2\nu-1}\Gamma^2(\nu)} \sum_{n=0}^{\infty} (\nu+n) \frac{\Gamma(2\nu+n)}{n!} \left|h_n^{\nu}\right|^2 \qquad (50)$$

Taking in (50) $\nu = \frac{q+1}{2}$ and substituting in (49) we get:

$$P_S = \frac{\omega^2\mu^2}{4\pi\eta} \sum_{q=2}^{\infty} \alpha_q \frac{2\pi}{2^q \Gamma^2(\frac{q+1}{2})} \cdot$$

$$\cdot \sum_{n=0}^{\infty} \left(\frac{q+1}{2}+n\right) \frac{\Gamma(q+n+1)}{n!} \left| h_n^{\frac{q+1}{2}} \right|^2 \qquad (51)$$

rearranging (51) we get:

$$P_S = \frac{\omega^2\mu^2}{4\pi\eta} \sum_{n=0}^{\infty} \sum_{q=2}^{\infty} \alpha_q \frac{\pi}{2^q \Gamma^2(\frac{q+1}{2})} (2n+q+1) \frac{(q+n)!}{n!} \left| h_n^{\frac{q+1}{2}} \right|^2 \qquad (52)$$

where $h_n^{\frac{q+1}{2}}$ is given in (29).

From (52) we see also that, in the general case of the broadside array, the radiated power consists of an infinite number of distinct modes.

By using (29) and the identity in (A-5) it may be shown from (52) that the total radiated power from one element is constant and independent of the position of the origin.

Case III: End fire Array (Fig. 3c) An array with radiators of circular pattern $\lambda(\theta)$, the axes of which is perpendicular to the axis of the array.

It may be shown[7] that the radiation pattern of this array is given by:

$$F(\theta,\varphi) = \lambda(\theta) \sum_{\ell=0}^{L} A_\ell e^{ikx_\ell \cos\varphi \sin\theta} \qquad (53)$$

where (θ,φ) are the angles in spherical coordinates. For θ = constant we have a similar expression to (2), and for φ = constant we have a similar expression as (4a). However, in this case the pattern is not circularly symmetric around the array axis, therefore it is a more complicated case.

Using expansion (5-b) in (53) with respect to ψ we get:

$$F(\theta,\psi)=\lambda(\theta)\sum_{n=-\infty}^{+\infty} i^n e^{in\psi}\sum_{\ell=0}^{L} A_\ell J_n(kx_\ell\sin\theta) \tag{54}$$

(54) may be rewritten as:

$$F(\theta,\psi)=\lambda(\theta)\sum_{n=-\infty}^{+\infty} i^n e^{in\psi} B_n(\theta) \tag{55a}$$

where: $$B_n(\theta)=\sum_{\ell=0}^{L} A_\ell J_n(kx_\ell\sin\theta) \tag{55b}$$

Taking the square of (55a):

$$|F(\theta,\psi)|^2=\lambda^2(\theta)\sum_{n=-\infty}^{+\infty}\sum_{m=-\infty}^{+\infty} i^n(-i)^m e^{i(n-m)\psi} B_n(\theta)B_m^*(\theta) \tag{56}$$

Substituting (56) in (34) and using the orthogonality properties:

$$\int_0^{2\pi} e^{i(n-m)\psi}d\psi=2\pi\,\delta_{n,m} \tag{57}$$

we get:

$$P_E=\frac{\pi^2\mu^2}{4\pi\eta}\sum_{n=-\infty}^{+\infty}\frac{1}{2}\int_0^{\pi}|B_n(\theta)|^2\,\lambda^2(\theta)\sin\theta d\theta \tag{58}$$

(58) shows that the radiated power of the endfire array consists of distinct modes. However, the relations between the magnitude of each mode and the elements of the array are more complicated because the pattern is not circular symmetric around the axis of the array.

It has been known[5] for quite a while that the electro-magnetic field, outside the sphere surrounding the sources, consists of distinct spherical modes. However, in this section we have shown a direct relation between the magnitude of each mode and the elements of a linear array.

3. The Radiated Power

In the following section we shall calculate the radiated power of the linear array. The total radiated power may be calculated in two ways:

a. Summation of the power radiated in each mode based on the equations given in Appendix A.

b. Direct integration of the radiation pattern.

Here we shall use the second, more direct method.

Case I. Basic Array (Fig. 3a)

In this case:

$$F(\theta,\psi) = \sum_{\ell=0}^{L} A_\ell e^{ikx_\ell \cos\theta} \tag{59}$$

From (59) we get:

$$|F(\theta,\psi)|^2 = \sum_{\ell=0}^{L}\sum_{m=0}^{L} A_\ell A_m^* e^{ikx_{\ell m}\cos\theta} \tag{60}$$

where: $x_{\ell m} = x_\ell - x_m$

Substituting (60) in (34) we get after simplification:

$$P_B = \frac{\omega^2\mu^2}{4\pi\eta}\sum_{\ell=0}^{L}\sum_{m=0}^{L} A_\ell A_m^* \frac{1}{2}\int_0^\pi e^{ikx_{\ell m}\cos\theta}\sin\theta d\theta \tag{61}$$

Calculating the integral in (61)

$$\frac{1}{2}\int_0^\pi e^{ikx_{\ell m}\cos\theta}\sin\theta d\theta = \frac{1}{2}\int_{-1}^{1} e^{ikx_{\ell m}y}dy = \frac{\sin kx_{\ell m}}{kx_{\ell m}} \tag{62}$$

(61) may be rewritten in the form:

$$P_B = \frac{\omega^2\mu^2}{4\pi\eta}\sum_{\ell=0}^{L}\sum_{m=0}^{L} A_\ell A_m^* I_B(x_{\ell m}) \tag{63}$$

where from (62):

$$I_B(x_{\ell m}) = \frac{\sin kx_{\ell m}}{kx_{\ell m}} \qquad x_{\ell m} = x_\ell - x_m \tag{64}$$

$I_B(x_{\ell m})$ will be called the "interaction coefficient" of the basic array.

Case II: Broadside Array (Fig. 3b)

In this case:

$$F(\theta, \varphi) = \lambda(\theta) \sum_{\ell=0}^{L} A_\ell e^{ikx_\ell \cos\theta} \tag{65}$$

From (65) we get:

$$\left| F(\theta,\varphi) \right|^2 = \lambda^2(\theta) \sum_{\ell=0}^{L} \sum_{m=0}^{L} A_\ell A_m^* e^{ikx_{\ell m}\cos\theta} \tag{66}$$

where: $x_{\ell m} = x_\ell - x_m$

Substituting (66) in (34) we get, after simplification:

$$P_S = \frac{\omega^2\mu^2}{4\pi\eta} \sum_{\ell=0}^{L} \sum_{m=0}^{L} A_\ell A_m^* \frac{1}{2} \int_0^\pi \lambda^2(\theta)\, e^{ikx_{\ell m}\cos\theta} \sin\theta d\theta \tag{67}$$

(67) may be rewritten as:

$$P_S = \frac{\omega^2\mu^2}{4\pi\eta} \sum_{\ell=0}^{L} \sum_{m=0}^{L} A_\ell A_m^* I_S(x_{\ell m}) \tag{68}$$

where $I_S(x_{\ell m})$ is the interaction coefficient of the broadside linear array and is given by:

$$I_S(x_{\ell m}) = \frac{1}{2} \int_0^\pi e^{ikx_{\ell m}\cos\theta} \lambda^2(\theta) \sin\theta d\theta \tag{69}$$

Stratton[9] gives the following integral relation:

$$i^n j_n(kR) P_n^m(\cos\beta) = \frac{1}{2} \int_0^\pi e^{ikR\cos\beta\cos\theta} J_m(kR\sin\beta\sin\theta) P_n^m(\cos\theta)\sin\theta d\theta \tag{70}$$

Substituting in (70) m=0 β=0 we get the relation:

$$i^n j_n(kR) P_n(1) = \frac{1}{2} \int_0^\pi e^{ikR\cos\theta} P_n(\cos\theta)\sin\theta d\theta \tag{71}$$

In order to transform (69) into the form of (71) we have to expand:

$$\lambda^2(\theta) = \sum_{s=0}^{\infty} \alpha_s P_s(\cos\theta) \qquad 0 \leq \theta \leq \pi \tag{72}$$

It may be done with the help of the orthogonality properties (18). Substituting (72) in (69), interchanging summation and integration signs, and using (71) we get:

$$I_S(x_{\ell m}) = \sum_{s=0}^{\infty} \alpha_s i^s P_s(1)\, j_s(kx_{\ell m}) \tag{73}$$

Case III: (Endfire Array (Fig. 3c)

In this case as in (53):

$$F(\theta,\psi) = \lambda(\theta) \sum_{\ell=0}^{L} A_\ell e^{ikx_\ell \sin\theta\cos\psi} \tag{74}$$

From (74) we get:

$$|F(\theta,\psi)|^2 = \lambda^2(\theta) \sum_{\ell=0}^{L} \sum_{m=0}^{L} A_\ell A_m^* e^{ikx_{\ell m}\sin\theta\cos\psi} \tag{75}$$

where: $x_{\ell m} = x_\ell - x_m$

Substituting (75) in (34) we get:

$$P_E = \frac{\omega^2\mu^2}{4\pi\eta} \sum_{\ell=0}^{L} \sum_{m=0}^{L} A_\ell A_m^* I_E(x_{\ell m}) \tag{76}$$

where $I_E(kx_{\ell m})$ is the interaction coefficient of the endfire linear array and given by:

$$I_E(x_{\ell m}) = \frac{1}{4\pi} \int_0^{\pi} \lambda^2(\theta)\sin\theta d\theta \int_0^{2\pi} e^{ikx_{\ell m}\sin\theta\cos\psi} d\psi \tag{77}$$

It is known[8] that :

$$J_o(z) = \frac{1}{2\pi} \int_0^{2\pi} e^{iz\cos\psi} d\psi \tag{78}$$

Using (78) in (77) we get:

$$I_E(x_{\ell m}) = \frac{1}{2} \int_0^{\pi} J_0(kx_{\ell m}\sin\theta)\ \lambda^2(\theta)\ \sin\theta d\theta \tag{79}$$

Substituting in (70) $m = 0$ $\beta = \frac{\pi}{2}$ we get the relation:

$$i^n j_n(kR)P_n(0) = \frac{1}{2} \int_0^{\pi} J_0(kR\sin\theta)P_n(\cos\theta)\sin\theta d\theta \tag{80}$$

expanding $\lambda^2(\theta)$ as in (72) and substituting in (79), we get, using (80):

$$I_E(x_{\ell m}) = \sum_{s=0}^{\infty} \alpha_s i^s P_s(0) j_s(kx_{\ell m}) \tag{81}$$

4. Interaction Coefficients and Gain

Let us summarize the results of the previous section as follows:

The total radiated power P of a linear array is given by:

$$P = \frac{\omega^2\mu^2}{4\pi\eta} \sum_{\ell=0}^{L} \sum_{m=0}^{L} A_\ell A_m^* I(x_{\ell m}) \tag{82}$$

The total radiated power has the same form for all cases of the linear array; the only difference we have is in the interaction coefficient.

In the general case, when each element has a circular pattern $\lambda(\theta)$ which is expanded, as in (72):

$$\lambda^2(\theta) = \sum_{s=0}^{\infty} \alpha_s P_s(\cos\theta) \qquad 0 \leq \theta \leq \pi \tag{83}$$

The interaction coefficients for the braodside and endfire arrays are given by (73), (81):

$$I_S(x_{\ell m}) = \sum_{s=0}^{\infty} \alpha_s i^s P_s(1) j_s(kx_{\ell m}) \tag{84a}$$

$$I_E(x_{\ell m}) = \sum_{s=0}^{\infty} \alpha_s i^s P_s(0)\, j_s(kx_{\ell m}) \tag{84b}$$

where $x_{\ell m} = x_\ell - x_m$

It may be shown[10] that:

$$P_n(1)=1 \quad P_{2n+1}(0)=0 \quad P_{2n}(0) = (-)^n \frac{(2n)!}{(2^n n!)^2} \tag{85}$$

Substituting (85) in (84) we get:

$$I_S(x_{\ell m}) = \sum_{s=0}^{\infty} \alpha_s i^s j_s(kx_{\ell m}) \tag{86a}$$

$$I_E(x_{\ell m}) = \sum_{s=0}^{\infty} \alpha_{2s} \frac{(2s)!}{(2^s s!)^2}\, j_{2s}(kx_{\ell m}) \tag{86b}$$

In the case of basic array with isotropic radiators:

$$\lambda(\theta)=1 \qquad \alpha_s = \delta_s = \begin{cases} 1 & s = 0 \\ 0 & s \neq 0 \end{cases} \tag{87}$$

Substituting (87) in either (86a) or (86b) we get:

$$I_B(x_{\ell m}) = j_o(kx_{\ell m}) \tag{88}$$

In the case of dipole elements we have, according to (83):

$$\lambda(\theta)=\sin\theta \quad \alpha_o = \frac{2}{3} \quad \alpha_2 = -\frac{2}{3} \tag{89}$$

Substituting (89) in (86) we get:

$$I_S^{(d)}(x_{\ell m}) = \frac{2}{3}\left[j_o(kx_{\ell m}) + j_2(kx_{\ell m})\right] \tag{90a}$$

$$I_E^{(d)}(x_{\ell m}) = \frac{2}{3}\left[j_o(kx_{\ell m}) - \frac{1}{2}\, j_2(kx_{\ell m})\right] \tag{90b}$$

From (88) and (90) we see that:

$$I_E^{(d)}(x_{\ell m}) + \frac{1}{2}\, I_S^{(d)}(x_{\ell m}) = I_B(x_{\ell m}) \tag{91}$$

It is shown by Stratton[9] that:

$$j_o(\rho) = \frac{\sin\rho}{\rho} \tag{92a}$$

$$j_2(\rho) = -\frac{\sin\rho}{\rho} + \frac{3}{\rho^2}\left[\frac{\sin\rho}{\rho} - \cos\rho\right] \tag{92b}$$

Substituting (92) in (88) and (90) we get:

$$I_B(x_{\ell m}) = \frac{\sin kx_{\ell m}}{kx_{\ell m}} \tag{93a}$$

$$I_S^{(d)}(x_{\ell m}) = \frac{2}{(kx_{\ell m})^2}\left[\frac{\sin kx_{\ell m}}{kx_{\ell m}} - \cos kx_{\ell m}\right] \tag{93b}$$

$$I_E^{(d)}(x_{\ell m}) = \frac{\sin kx_{\ell m}}{kx_{\ell m}} - \frac{1}{(kx_{\ell m})^2}\left[\frac{\sin kx_{\ell m}}{kx_{\ell m}} - \cos kx_{\ell m}\right] \tag{93c}$$

In case we have a single element and therefore $kx_{\ell m}=0$ and since

$$j_o(0) = 1 \qquad j_{s>o}(0)=0 \tag{94}$$

we get from (86):

$$I_S(0) = I_E(0)=\alpha_o \tag{95}$$

(95) is obvious physically, since, in case we have one radiator only, it radiates the same power in both cases.

From (87), (89) and (95) we get:

$$I_B(0)=1 \qquad I_S^{(d)}(0)=I_E^{(d)}(0) = \frac{2}{3} \tag{96}$$

The interaction coefficients for the basic array, and the linear array with dipole elements are drawn in Fig. 4

In case we have the spacing between the radiators equal to multiples of half wavelength we have

$$kx_{\ell m} = k(x_\ell - x_m) = \frac{2\pi}{\lambda}(\ell-m)\frac{\lambda}{2} = (\ell-m)\pi \tag{97}$$

In this case (93a) becomes:

$$I_B^{(\frac{\lambda}{2})}(x_{\ell m}) = I_B\left[(\ell-m)\pi\right] = \frac{\sin(\ell-m)\pi}{(\ell-m)\pi} = \delta_{\ell,m} = \begin{cases} 1 & \ell=m \\ 0 & \ell\neq m \end{cases} \tag{98}$$

and the radiated power in (82) becomes:

$$P_B^{(\frac{\lambda}{2})} = \frac{\omega^2\mu^2}{4\pi\eta}\sum_{\ell=0}^{L}|A_\ell|^2 \tag{99}$$

The total power radiated in this case is the sum of the powers radiated by each element alone.

This is not the case in a physically realizable array of dipoles, since the zeros in Fig. 4 are not equally distributed for dipoles as in the case of the basic array. However, we see from Fig. 4 that if we take a broadside array with dipoles spaced equally at 0.72λ, we get approximately the property

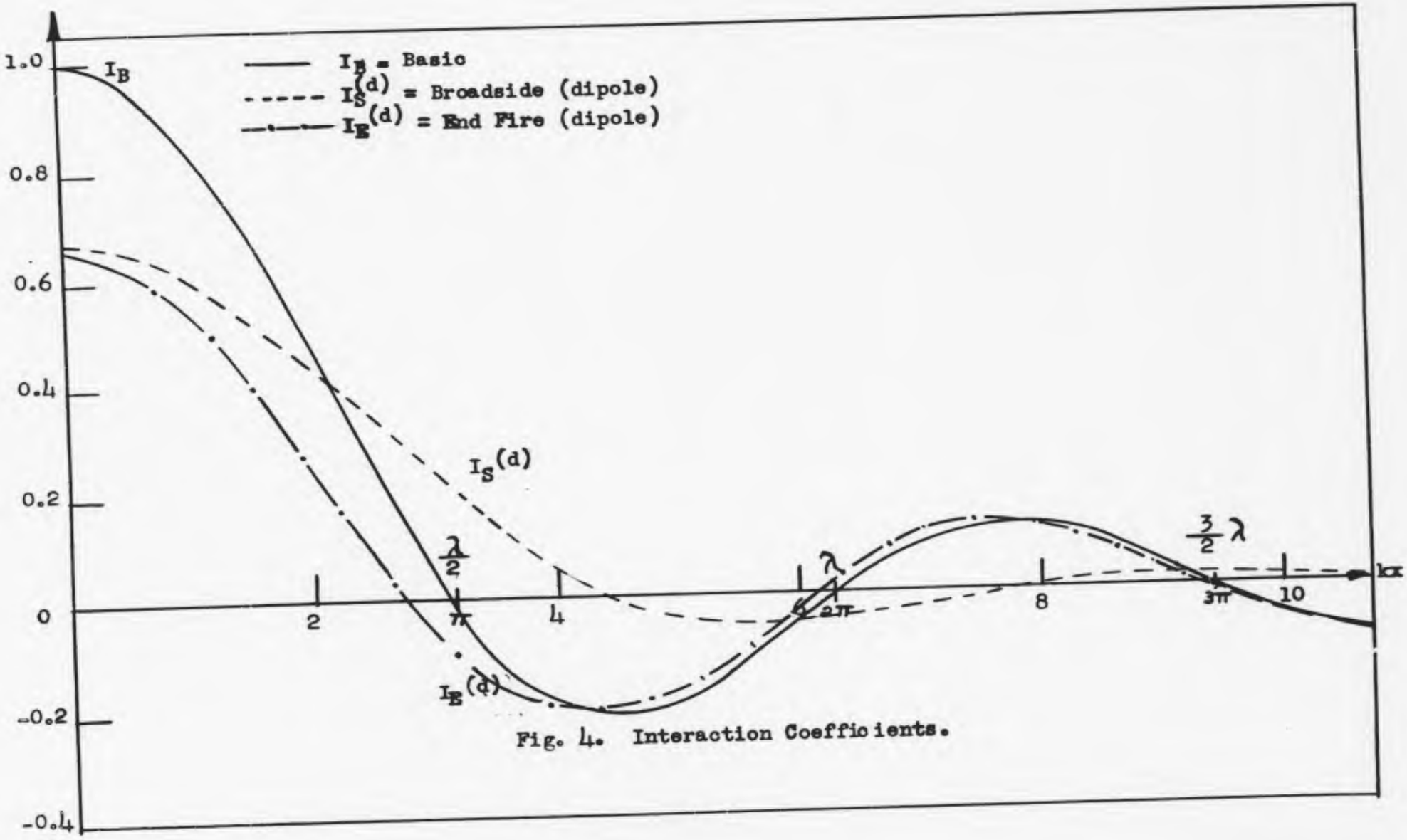

Fig. 4. Interaction Coefficients.

in(99). This is due in this case to the fact that the interaction coefficient is very small between the two far elements.

The gain G of an array may be defined as

$$G = \frac{4\pi R^2 \frac{1}{\eta} |E(\theta,\varphi)|^2}{P} \tag{100}$$

where the denominator gives the actual radiated power, and the numerator gives the radiated power as if the whole radiated field around the array were equal to the field in the direction of the main lobe $(\theta_o; \varphi_o)$. From (32) we see that:

$$4\pi R^2 \frac{1}{\eta} |E(\theta_o;\varphi_o)|^2 = \frac{\omega^2\mu^2}{4\pi\eta} |F(\theta_o;\varphi_o)|^2 \tag{101}$$

In the case of broadside array $\theta_o = \frac{\pi}{2}$ and from (65):

$$F(\tfrac{\pi}{2};\varphi) = \lambda(\tfrac{\pi}{2}) \sum_{\ell=0}^{L} A_\ell \tag{102a}$$

In the case of endfire array $\varphi_o = \frac{\pi}{2}$; $\theta_o = \frac{\pi}{2}$ and from (74)

$$F(\tfrac{\pi}{2};\tfrac{\pi}{2}) = \lambda(\tfrac{\pi}{2}) \sum_{\ell=0}^{L} A_\ell \tag{102b}$$

Substituting (102) in (101) and assuming normalization $\lambda(\frac{\pi}{2}) = 1$ we get:

$$4\pi R^2 \frac{1}{\eta} |E(\theta_o;\varphi_o)|^2 = \frac{\omega^2\mu^2}{4\pi\eta} \left| \sum_{\ell=0}^{L} A_\ell \right|^2 \tag{103}$$

Substituting (82) and (103) in 100) we get:

$$G = \frac{\left| \sum_{\ell=0}^{L} A_\ell \right|^2}{\sum_{\ell=0}^{L} \sum_{m=0}^{L} A_\ell A_m^* I(x_{\ell m})} \tag{104a}$$

(104a) may be rewritten in a more symmetric form:

$$G = \frac{\sum_{\ell=0}^{L} \sum_{m=0}^{L} A_\ell A_m^*}{\sum_{\ell=0}^{L} \sum_{m=0}^{L} A_\ell A_m^* I(x_{\ell m})} \tag{104b}$$

In case we have only one radiator (104) becomes, due to (95):

$$G^I = \frac{1}{I(0)} = \frac{1}{\alpha_o} \tag{105}$$

and from (96) we get:

$$G_B^I = 1 \quad G_S^{I(d)} = G_E^{I(d)} = \frac{3}{2} \tag{106}$$

The gain of a uniform radiator is 1 and that of a dipole is 1.5.

5. Stored Energy and Figure of Merit

If we solve the total field of a radiator, we see that besides the radiated field, there are also non-radiated fields which represent the stored energy around the radiator. The reason for this is that the radiated fields by themselves do not satisfy Maxwell's equations. As an example, let us write down the field of an electric dipole :

$$E_r = \frac{1}{2} A\left(\frac{1}{\rho^3} + \frac{i}{\rho^2}\right) \cos\theta e^{i(\omega t-\rho)} \tag{107a}$$

$$E_\theta = A\left(\frac{1}{\rho^3} + \frac{i}{\rho^2} - \frac{1}{\rho}\right) \sin\theta e^{i(\omega t-\rho)} \tag{107b}$$

$$H_\varphi = \frac{A}{\eta}\left(\frac{i}{\rho^2} - \frac{1}{\rho}\right) \sin\theta e^{i(\omega t-\rho)} \tag{107c}$$

where: $\eta = \sqrt{\frac{\mu}{\varepsilon}}$ $\qquad \rho = kr = 2\pi \frac{r}{\lambda}$

$A = \frac{k^3}{4\pi} p_o$ amplitude of dipole

We see from (107) that when $\rho > 1$ the radiated field becomes dominant.

Let us put a set of dipoles in a linear array form as in Fig. 5. There is a certain interaction between the dipoles and we assume that <u>after</u> they have interacted each dipole will have an amplitude A_ℓ. We divide the space around the array into three ranges I, II, II, where range III includes the immediate space around each dipole.

Let us denote the stored energy in each range by U_{SI}; U_{SII}; U_{SIII}, and the total stored energy will be:

$$U_S = U_{SI} + U_{SII} + U_{SIII} \tag{108}$$

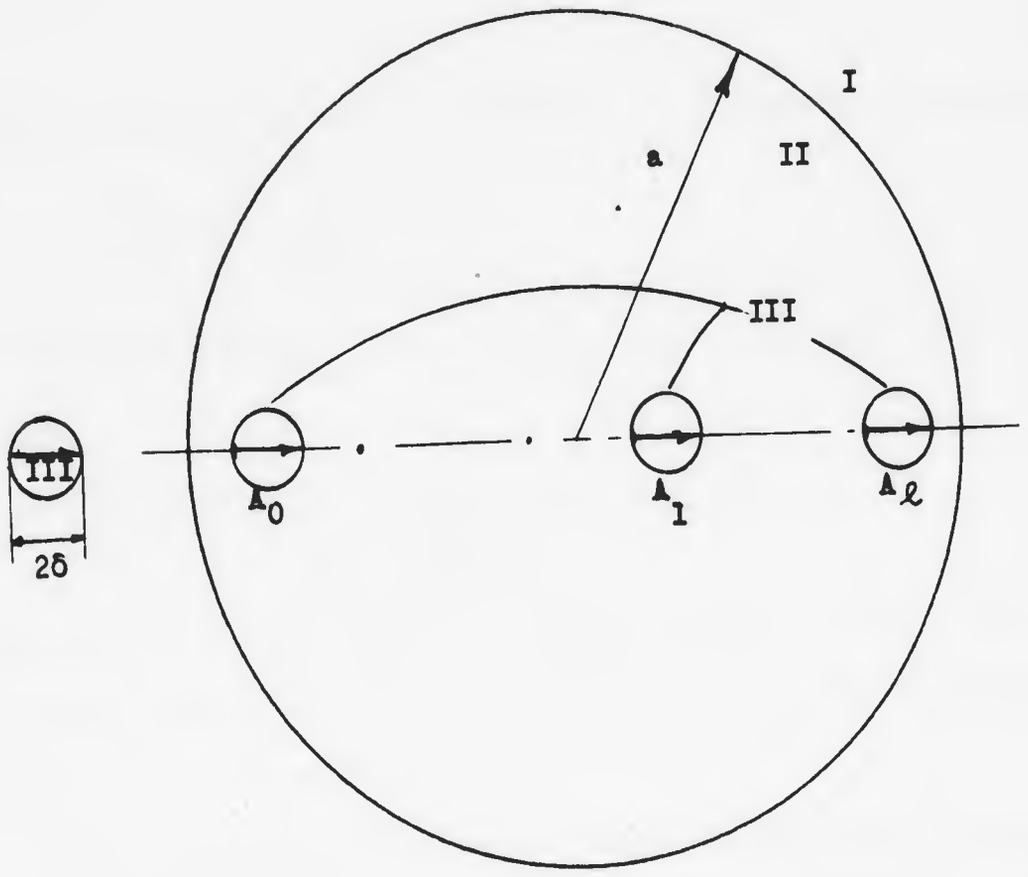

Fig. 5. Stored Energy.

U_{SI} is stored energy in form of a traveling wave and has been calculated by Chu[5].

Let us now calculate U_{SIII} around one dipole. Since the dipole is infinitely small, it may be surrounded by a sphere of radius $\delta \to 0$. The total electric energy around the dipole will be given by:

$$\int_0^{2\pi} d\varphi \int_0^{\pi} \sin\theta d\theta \int_{\delta\to 0}^{\alpha} R^2 \varepsilon \left[|E_\theta|^2 + |E_r|^2 \right] dR \qquad (109)$$

The field in the immediate space around the dipole includes the fields in (107) plus a constant field due to all the other dipoles. Substituting (107) and a constant field in (109) we see that, since $\delta \to 0$, the result will go to infinity as $\frac{|A|^2}{\delta^3}$. The stored energy will be infinitely large which should have been expected since the dimensions of the radiator are zero.

However, since physical radiators have finite dimensions we can write:

$$U_S \geq U_{SIII} \propto \sum_{\ell=0}^{L} |A_\ell|^2 \tag{110}$$

for (L+1) radiators. U_{SIII} or $U_{SIII} + U_{SI}$ will be the lower bound of the stored energy.

Let us define Q factor for the array as follows:

$$Q = \omega \frac{U_{SIII}}{P} \tag{111}$$

Q factor is similar to the Q of a resonance circuit. When Q is high there is a resonance in only a narrow band of frequencies. As Q becomes smaller, the resonant circuit becomes broadband.

Since we would like the array to radiate as much power as possible for the same amount of stored energy, i.e. to be as broadband as possible, we try, in the case of the array, to make the Q factor as low as possible.

Let us substitute in (111) both (110) and (82). We get:

$$Q \propto \frac{\sum_{\ell=0}^{L} |A_\ell|^2}{\sum_{\ell=0}^{L} \sum_{m=0}^{L} A_\ell A_m^* I(x_{\ell m})} \tag{112}$$

(112) may be rewritten with a coefficient C as the constant of proportionality for a given array:

$$Q = C \frac{\sum_{\ell=0}^{L} |A_\ell|^2}{\sum_{\ell=0}^{L} \sum_{m=0}^{L} A_\ell A_m^* I(x_{\ell m})} \tag{113}$$

Let us find now what the constant of proportionality C is. If we take in (113) only one element A_o in the array we get:

$$Q^I = C \frac{|A_o|^2}{|A_o|^2 I(0)} = \frac{C}{I(0)} \tag{114}$$

where Q^I is the Q factor of one radiator by itself.

From (105) and (114) we get:

$$C = Q^I I(0) = \frac{Q^I}{G^I} \tag{115}$$

where G^I is the gain of each element by itself.

Substituting (115) in (113) we get:

$$Q = \frac{Q^I}{G^I} \frac{\sum_{\ell=0}^{L} |A_\ell|^2}{\sum_{\ell=0}^{L} \sum_{m=0}^{L} A_\ell A_m^* I(x_{\ell m})} \tag{116}$$

We see that the properties of one element by itself have to be known in order to calculate the Q factor for the whole array of similar elements.

Usually broadband arrays with maximum gain are desired. In other words we want Q→minimum and G→maximum. In order to take both into account, let us consider the ratio $\frac{Q}{G}$. From (104a), (116) we get:

$$\frac{Q}{G} = \frac{Q^I}{G^I} \frac{\sum_{\ell=0}^{L} |A_\ell|^2}{\left| \sum_{\ell=0}^{L} A_\ell \right|^2} \tag{117}$$

We want to minimize $\frac{Q}{G}$; (117) may be rewritten as:

$$\xi = \frac{Q/Q^I}{G/G^I} = \frac{\sum_{\ell=0}^{L} |A_\ell|^2}{\left| \sum_{\ell=0}^{L} A_\ell \right|^2} \tag{118}$$

ξ in (118) is called "figure of merit" of the array and we want to make it as small as possible.

Although we obtained the gain G in the previous section for a symmetric sharp beam, the definition of the figure of merit ξ is quite general and may be used for any pattern in any linear array. In the case of a single element A_o:

$$\xi^I = 1 \tag{119}$$

When a very large gain from a finite length of the array, is required, as

in the case of a super-gain array, we shall get ξ very large and the array would not be effective (the gain per unit of stored energywill be very small.)

Suppose we have an array with L+1 elements. Let us find what distribution of currents A_ℓ along the elements gives us minimum ξ. A_ℓ is a complex number in general.

Let us first hold the numerator in (118) constant and look at the denominator. It will be maximum when all A_ℓ will have the same phase. Then let us hold the denominator constant and look at the numerator. According to the identity

$$x^2 + y^2 = \frac{(x+y)^2}{2} + \frac{(x-y)^2}{2} \tag{120}$$

we see that the numerator will be minimum if all the elements have equal amplitude. Therefore:

$$\xi = \min. = \frac{1}{L+1} \quad \text{when } A_o = A_\ell \tag{121}$$

The figure of merit of the array will be minimum when all the currents in each element of the array are equal and in phase. The array has the best figure of merit when we have equal aperature distribution.

In order to compare the figure of merit of arrays with differing numbers of elements, we can define a normalized figure of merit ξ_N such that:

$$\xi_N = (L+1) \frac{\sum_{\ell=0}^{L} |A_\ell|^2}{\left|\sum_{\ell=0}^{L} A_\ell\right|^2} \tag{122}$$

where $\xi_N \geq 1$ $\qquad\qquad$ $\xi_N^I = 1$

A basic array, having elements separated by multiples of a half wavelength and with the interaction coefficient given by (98), will have the gain from (104a);

$$G_B\left(\frac{\lambda}{2}\right) = \frac{\left|\sum_{\ell=0} A_\ell\right|^2}{\sum_{\ell=} |A_\ell|^2} \tag{123}$$

which was the case considered by Woodward and Lawson[4].

The Q factor of an array of this type will be, from (116);

$$Q_B^{(\frac{\lambda}{2})} = Q^I \tag{124}$$

Since the gain of a uniform radiator is 1. The Q factor of the whole array will be equal to the Q factor of each element by itself.

From (118) and (123) we can see that in this particular case we have a new definition for the figure of merit.

$$\sum_B^{(\frac{\lambda}{2})} \frac{1}{Q_B(\frac{\lambda}{2})} \tag{125}$$

6. Examples

In this section we shall give the results of two examples which have been calculated using the above theory.

Example I: We want to produce the pattern:

$$F(\phi) = 32 \cos^4 \phi \tag{126}$$

by 5 elements (See Fig. 6). The array is symmetric, its length is fixed 2λ, and we vary two of the inner elements. Expanding (126) in a complex Fourier series (7a) we get the coefficients:

$$f_0 = 12 \quad f_2 = 8 \quad f_4 = 2 \quad f_{2n\geq 6} = 0 \tag{127a}$$

$$f_{2n+1} = 0 \tag{127b}$$

Since the array is symmetric, let us take the origin at A_0, and since

$$J_n(-x) = (-)^n J_n(x) \tag{128}$$

by taking

$$A_{-1} = A_1 \qquad A_{-2} = A_2 \tag{129}$$

we get (127b) immediately. From (8), (127a) and (129) we get:

$$A_1 J_4(kx) + A_2 J_4(2\pi) = 1 \tag{130a}$$

$$A_1 J_2(kx) + A_2 J_2(2\pi) = 4 \tag{130b}$$

$$A_1 J_0(kx) + A_2 J_0(2\pi) = 6 - \frac{1}{2} A_0 \tag{131}$$

Taking from the tables:

$$J_0(2\pi) = 0.220 \quad J_2(2\pi) = -0.287 \quad J_4(2\pi) = 0.316 \tag{132}$$

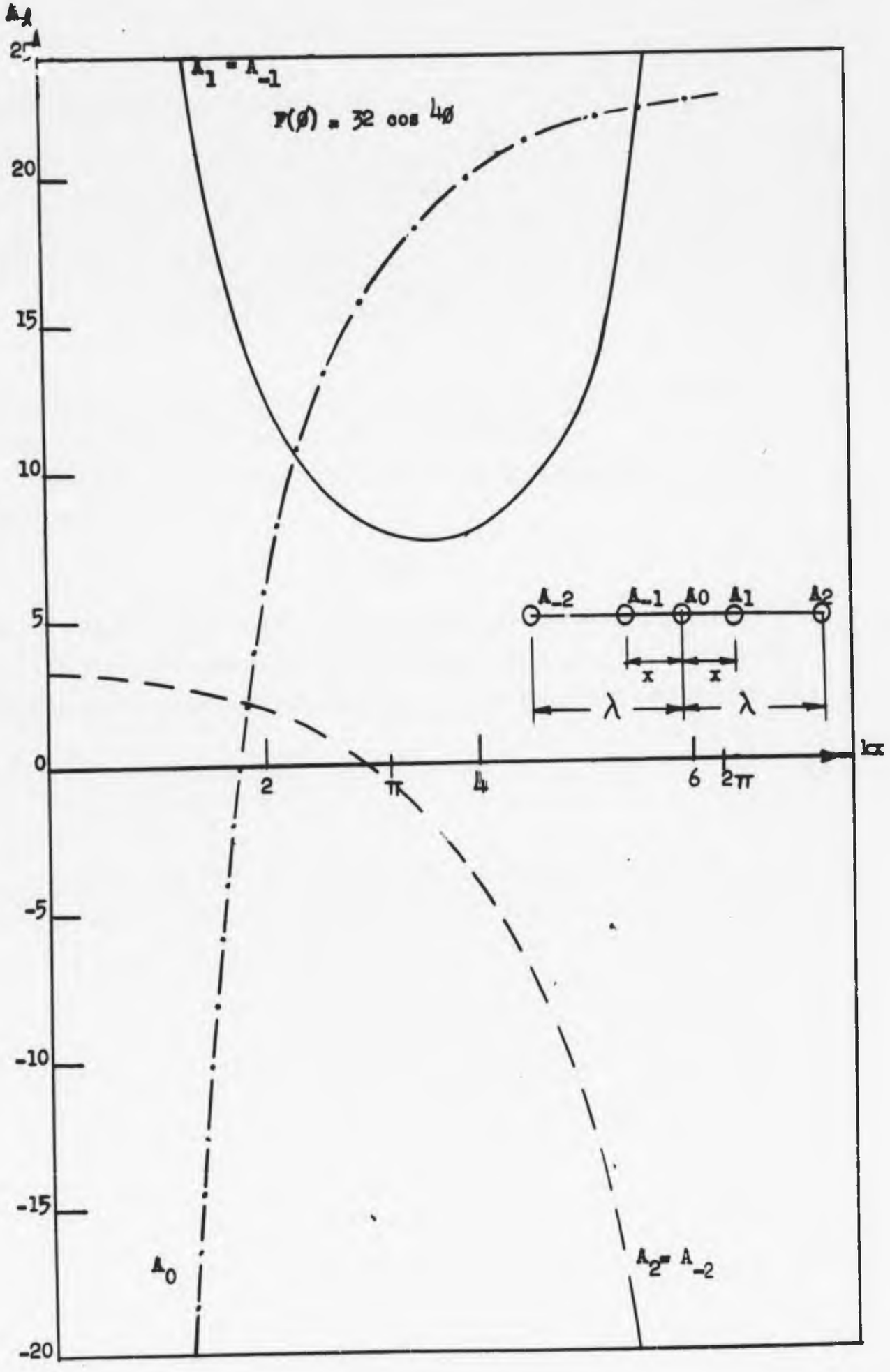

Fig. 6. Five Element Array

We get from (130) and (132):

$$A_1 = \frac{1.551}{0.316J_2(kx) + 0.287\ J_4(kx)} \tag{133a}$$

$$A_2 = \frac{J_2(kx) - 4J_4(kx)}{0.316J_2(kx) + 0.287J_4(kx)} \tag{133b}$$

Substituting those values in (131) we can get A_o. In Fig. 6 we have the results in a graphical form, with kx as the variable.

The most interesting point in Fig. 6 is $kx_o=2.9$ where $A_2=0$. This is the point where we have:

$$J_2(kx_o) - 4J_4(kx_o)=0 \tag{134}$$

In this case of separation we can eliminate the two outer radiators.

In Fig. 7 we have shown the coefficients of the higher terms of the Fourier series as calculated from (8). It may be proved easily that:

$$\lim_{\substack{n\to\infty \\ n\gg z}} \frac{J_{n+1}(z)}{J_n(z)} = \frac{z}{2n} \tag{135}$$

From (135) we see that according to (8), the higher order coefficients of the Fourier series vanish very rapidly. In Fig. 8 we have shown the figure of merit ξ calculated from (118).

$$F(\phi) = 32 \cos 4\phi = 2e^{i14\phi} + 8e^{i12\phi} + 12 + 8e^{-i12\phi} + 2e^{-i14\phi}$$

f_n $\quad f_o = 12 \quad f_2 = 8 \quad f_4 = 2 \quad f_{2n \geq 6} = 0 \quad f_{2n+1} = 0$

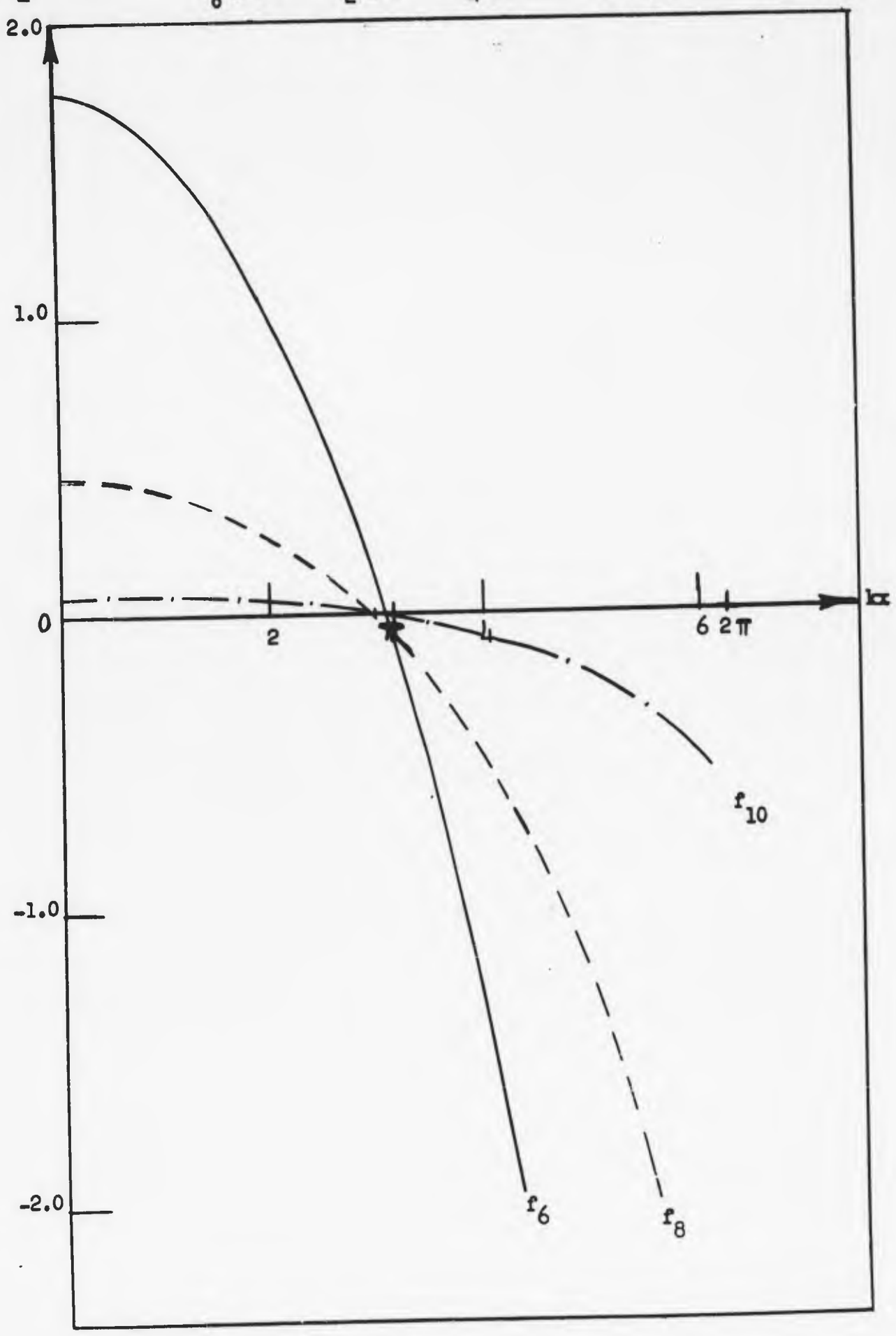

Fig. 7. Higher Order Fourier Coefficients.

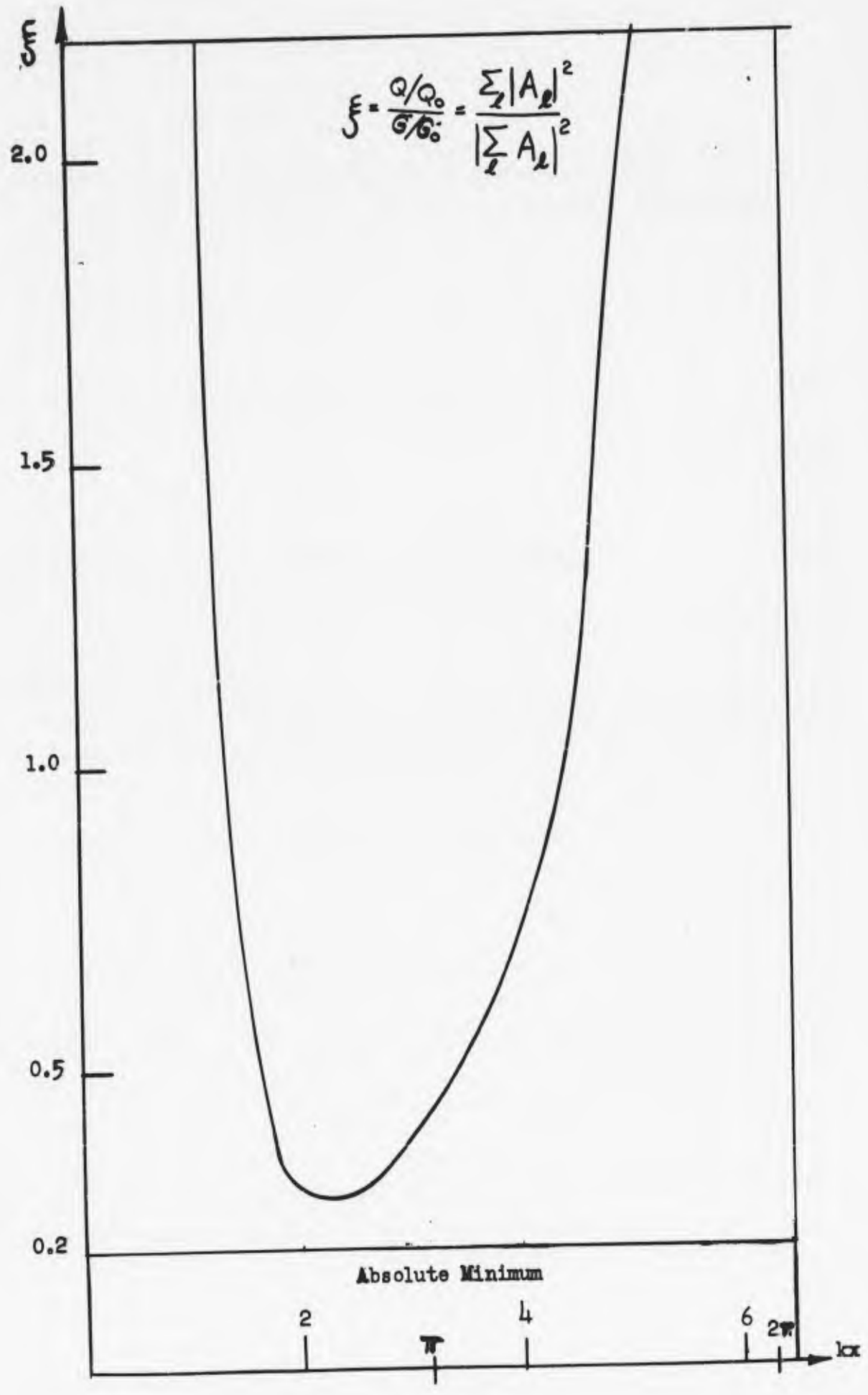

Fig. 8. Figure of Merit.

Example II: We want to approximate the pattern

$$F(\phi) = 2^{10}\cos^{10}\left(\frac{\pi}{2}\sin\phi\right) \tag{136}$$

The pattern in (136) is obtained exactly by a binomial array of 11 elements (Fig. 9a). We shall try to get the same pattern by only 7 elements and a shorter array(Fig. 9b).

By expanding (136) in a complex Fourier series (7a) or by using (8) we get:

$$\frac{1}{2} f_{2n} = J_{2n}(5\pi) + 10J_{2n}(4\pi) + 45J_{2n}(3\pi) + 120J_{2n}(2\pi) + 210J_{2n}(\pi) \tag{137a}$$

$$f_{2n+1} = 0 \tag{137b}$$

$$\frac{1}{2} f_o = 126 + J_o(5\pi) + 10J_o(4\pi) + 45J_o(3\pi) + 120J_o(2\pi) + 210J_o(\pi) \tag{138}$$

Table II gives the corresponding coefficients as calculated from the tables according to (137) (138).

To get the same coefficients by a 7 element array (Fig.9b) with non-equidistant distribution the following equations have to be solved:

$$\frac{1}{2} f_{2n} = A_3 J_{2n}(kx_3) + A_2 J_{2n}(kx_2) + A_1 J_{2n}(kx_1) \tag{139}$$

$$n \geqslant 1$$

$$\frac{1}{2} f_o = \frac{A_o}{2} + A_3 J_o(kx_3) + A_2 J_o(kx_2) + A_1 J_o(kx_1) \tag{140}$$

From (139) we have to find $(A_1; A_2; A_3)$ and $(x_1; x_2; x_3)$ which will give the same coefficients as in (137); we shall use semigraphical methods based on the curves for Bessel functions in Fig. 10 and their ratios in Fig. 11.

In Fig. 10 we have shown the range where each element would be. The exact position of each element will be found by method of trial and error, starting from assumed position of the outside element A_3.

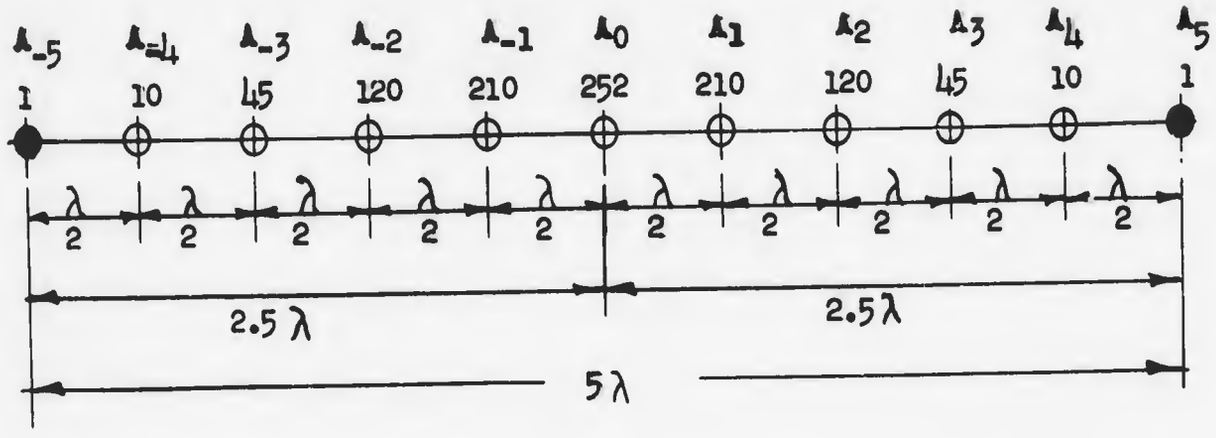

Fig. 9a. Binomial Array-Exact.

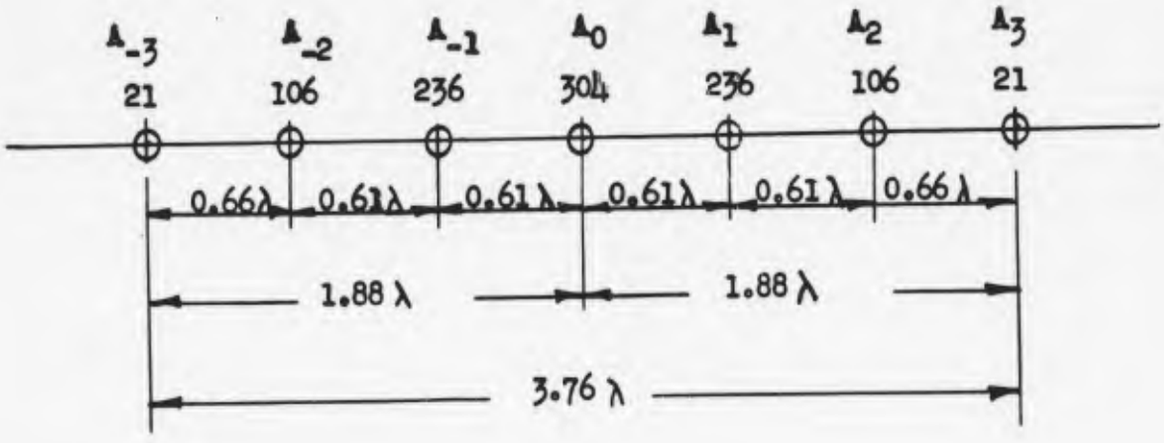

Fig. 9b. Binomial Array-Approximate.

$$F(\phi) = 2^{10} \cos^{10} \left(\frac{\pi}{2} \sin\phi\right)$$

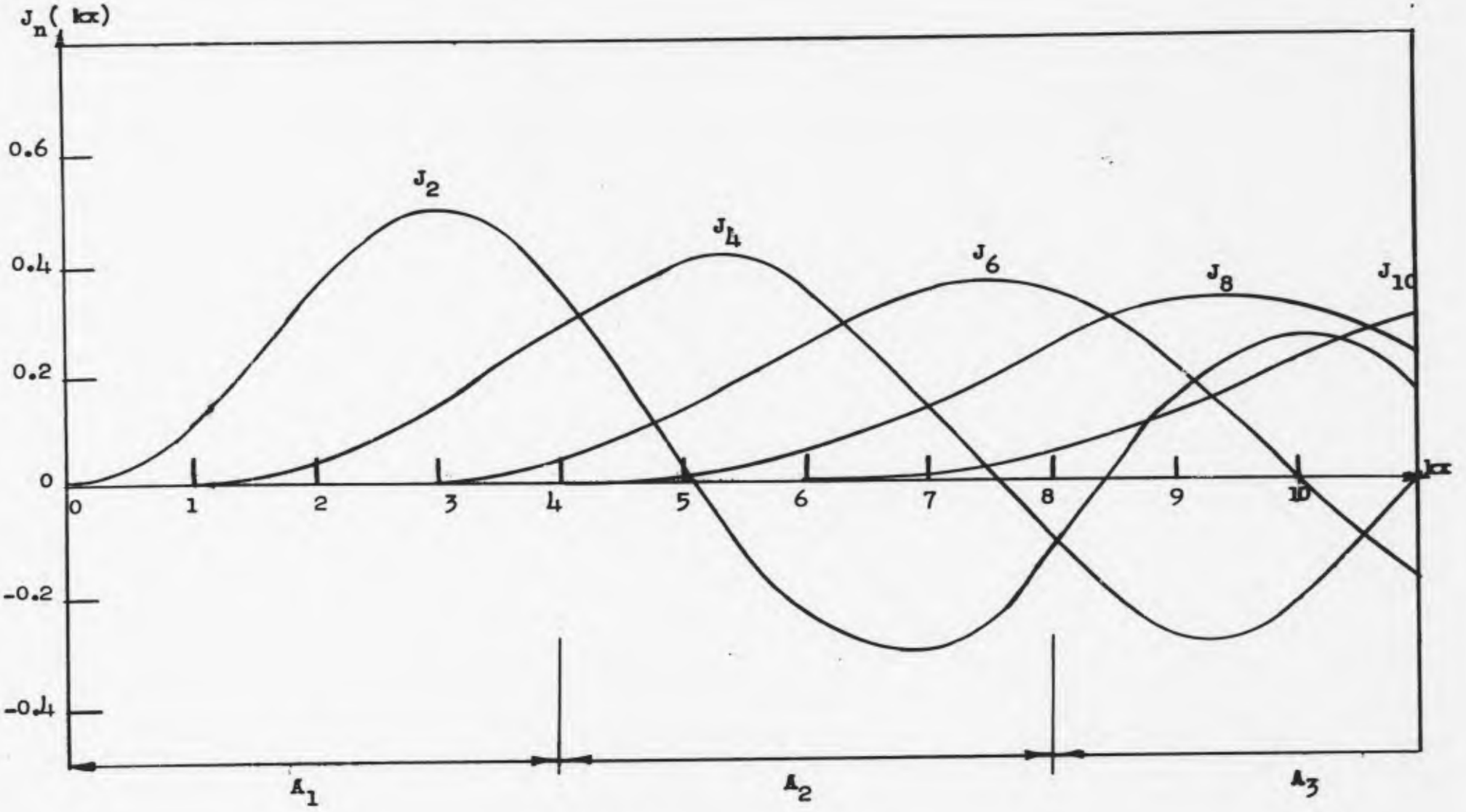

Fig. 10. Bessel Functions.

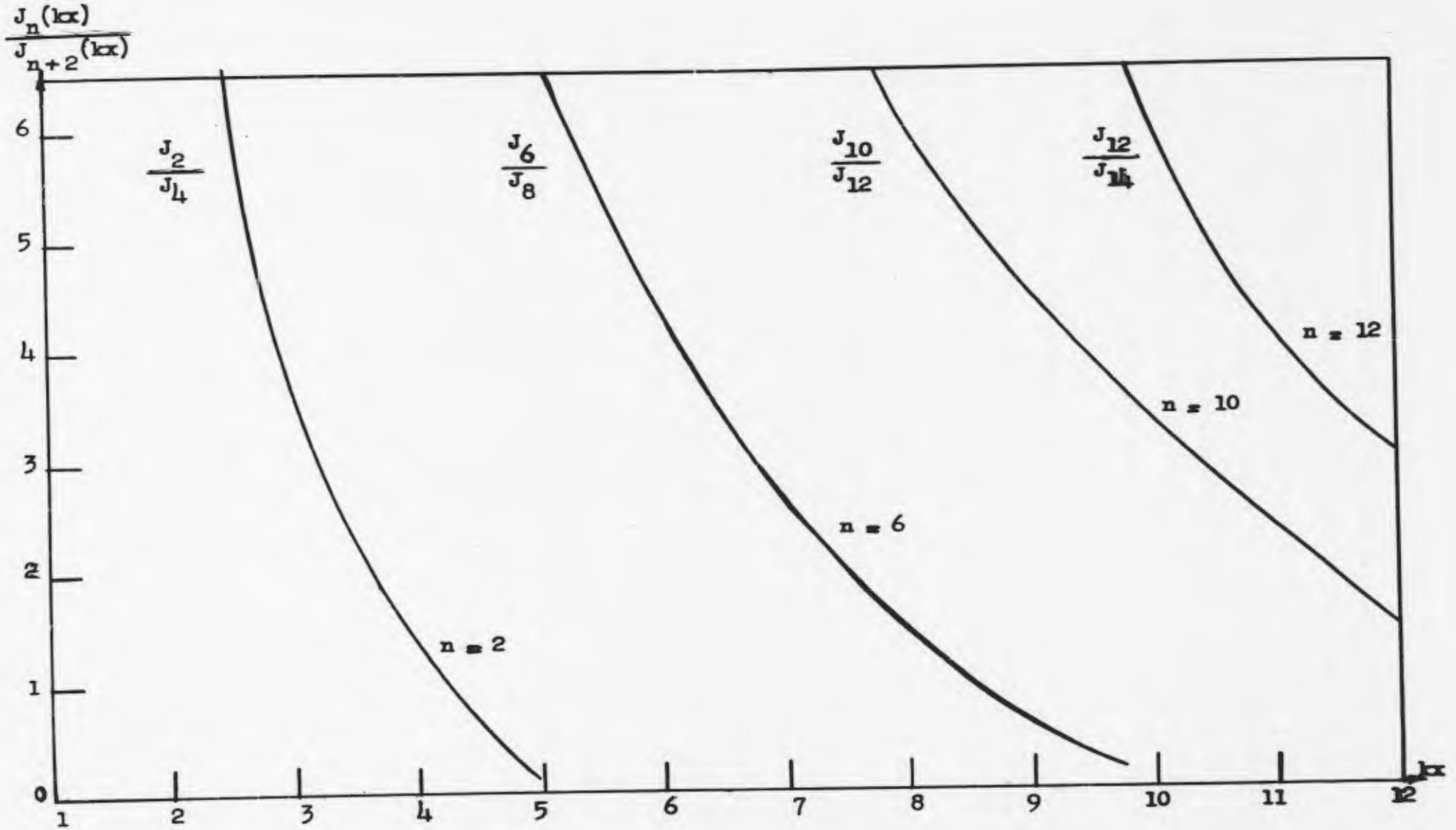

Fig. 11. Bessel Functions Ratios.

The first rough approximation may be made by assuming that A_1 contributes only to modes (2,4); A_2 contributes only to modes (2,4,6,8); A_3 contributes to all the modes including the other higher modes (10, 12, 14, . . .). The position of A_3 will have to be in such a position that $J_{10}(kx)$ is not too small, or, the required amplitude of A_3 will be too high; we will get high currents with alternate signs and the figure of merit ξ will be very large. By choosing the position of A_3 and with the above approximation, we can find from Fig. 11 the positions of A_2 and A_1. It is seen easily from the corresponding matrix relations. By corrections to these rough assumptions, the final result may be found. It may be extended to more elements, although the corrections of the rough approximation are then more difficult.

The results are tabulated in Table II and Fig. 9b. The error is less than 1°/o compared to the maximum of the pattern.

We can take the binomial array in Fig. 9a without the two outside elements, to produce the pattern in (136) with less than 1°/o error. In Table III we have compared the qualities of the three arrays which produce (136); the first one will be the exact binomial array; the second one will be our non-equidistant array; the third one will be the binomial array without the outside elements.

We see from the above example that we need fewer elements and get better performance in an array, if we add the distribution of the elements along the axis of the array as a variable of the design. Although the calculations are difficult at first, they may be simplified when more experience is acquired.

Table II: Non-Equi-Distant Approximate Binomial-Array

A_ℓ	kx_ℓ	x_ℓ	$J_0(kx_\ell)$	$J_2(kx_\ell)$	$J_4(kx_\ell)$	$J_6(kx_\ell)$	$J_8(kx_\ell)$
304	0	0 λ	1.0000	0	0	0	0
236	3.8	0.606 λ	-0.4026	0.4093	0.2507	0.0383	0.0028
106	7.7	1.223 λ	0.2346	-0.1875	-0.0297	0.3516	0.1940
21	11.8	1.881 λ	0.0020	-0.0413	0.1523	-0.2498	0.0849
Coefficient Required $\frac{1}{2}f_n$			82.0	75.6	59.5	39.9	22.7
Coefficient Achieved $\frac{1}{2}f_n$			82.0	75.8	59.4	41.2	22.9

A_ℓ	kx_ℓ	$J_{10}(kx_\ell)$	$J_{12}(kx_\ell)$	$J_{14}(kx_\ell)$	$J_{16}(kx_\ell)$	$J_{18}(kx_\ell)$	$J_{20}(kx_\ell)$
236	3.8	0.00012	-	-	-	-	-
106	7.7	0.04690	0.00670	0.00065	0.00004	-	-
21	11.8	0.30270	0.18020	0.05660	0.01160	0.00170	0.00019
Required $\frac{1}{2}f_n$		10.9	4.4	1.5	0.4	0.1	0.02
Achieved $\frac{1}{2}f_n$		11.3	4.5	1.3	0.24	0.035	0.004

Table III

Comparison between Arrays

$$F(\phi) = 2^{10} \cos^{10}\left(\frac{\pi}{2}\sin\phi\right)$$

Method / Performance	Exact	Approximate (Error<1°/o)	
		Non-Equi-Distant	Equi-Distant
No. of Fig.	9a	9b	9a
No. of Elements	11	7	9
Length of Array	5λ	3.76λ	4λ
Maximum Ratio of Currents	1:252	1:14.4	1:25.2
Figure of Merit ξ	0.175	0.214	0.175
Normalized Figure of Merit ξ_N	1.93	1.49	1.57

7. Analysis of the Array

By the analysis of an array we understand the problem of finding the relative magni ..des and phases of currents in an actual physical array for which we can measure the radiation pattern. The far zone pattern may be measured in phase and in amplitude or in amplitude alone. The latter measurement, of amplitude only, is the most usual one since it is much simpler to measure.

Starting from (4a) we take:

$$F(\phi) = \sum_{\ell=0}^{L} A_\ell \, e^{ikx_\ell \sin\phi} \tag{141}$$

$F(\phi)$ may be found by dividing the actual pattern by the pattern of a single element. $F(\phi)$ may be expanded as a complex Fourier series as in (7a) and then relation (8) holds:

$$f_n = \sum_{\ell=0}^{L} A_\ell \, J_n (kx_\ell) \tag{142a}$$

If we measure both amplitude and phase in the analysis problem we can find f_n. Since the distribution of the elements along the axis of the array x_ℓ may be measured, the only unknown in (142) is A_ℓ. It may be solved as (L+1) equations with (L+1) unknown, and the formal solution may be written as in (13):

$$\left[A\right] = \left[J\right]^{-1} \cdot \left[f\right] \tag{142b}$$

When only the amplitude of the pattern is measured, the solution is more complicated. Rewriting (141) in terms of explicit quantities we get:

$$F(\phi) = \sum_{\ell=0}^{L} (A_\ell + iB_\ell) \, e^{ikx_\ell \sin\phi} \tag{143a}$$

where A_ℓ, B_ℓ are real numbers. The conjugate of it is:

$$F^*(\phi) = \sum_{m=0}^{L} (A_m - iB_m) \, e^{-ikx_m \sin\phi} \tag{143b}$$

From (143) we get:

$$|F(\phi)|^2 = F(\phi)\cdot F^*(\phi) = \sum_{\ell=0}^{L}\sum_{m=0}^{L} (A_\ell + iB_\ell)(A_m - iB_m)\, e^{ikx_{\ell m}\sin\phi} \tag{144}$$

where $x_{\ell m} = x_\ell - x_m$. $|F(\phi)|^2$ or $|F(\phi)|$ is the magnitude when we measure the amplitude of the pattern only. Expanding $|F(\phi)|^2$ in a complex Fourier series:

$$|F(\phi)|^2 = \sum_{n=-\infty}^{+\infty} f_n\, e^{in\phi} \tag{145}$$

and using (5a) in (144), comparing with (145) we get:

$$f_n = f_n^R + if_n^i = \sum_{\ell=0}^{L}\sum_{m=0}^{L} J_n(kx_{\ell m})\cdot \cdot\left[(A_\ell A_m + B_\ell B_m) + i\,(A_m B_\ell - A_\ell B_m)\right] \tag{146}$$

Let us define:

$$C_{\ell m} = A_\ell A_m + B_\ell B_m \tag{147a}$$

$$D_{\ell m} = A_m B_\ell - A_\ell B_m \tag{147b}$$

and (146) becomes:

$$f_n^R = \sum_{\ell=0}^{L}\sum_{m=0}^{L} C_{\ell m}\, J_n(kx_{\ell m}) \tag{148a}$$

$$f_n^i = \sum_{\ell=0}^{L}\sum_{m=0}^{L} D_{\ell m}\, J_n(kx_{\ell m}) \tag{148b}$$

From (147) we see that:

$$C_{\ell m} = C_{m\ell} \qquad C_{\ell\ell} = A_\ell^2 + B_\ell^2 \tag{149a}$$

$$D_{\ell m} = -D_{m\ell} \qquad D_{\ell\ell} = 0 \tag{149b}$$

using the identity:

$$J_n(-z) = (-)^n \; J_n(z) \tag{150}$$

and (149) we get for (148) the following since $x_{\ell m} = -x_{m\ell}$:

n = odd

$$f_n^R = 0 \tag{151a}$$

$$f_n^i = 2 \sum_{\ell>}^{L} \sum_{m=0}^{L} D_{\ell m} J_n(kx_{\ell m}) \tag{151b}$$

n= even

$$f_n^i = 0 \tag{152a}$$

$$f_n^R = 2 \sum_{\ell>}^{L} \sum_{m=0}^{L} C_{\ell m} J_n(kx_{\ell m}) + \sum_{\ell=0}^{L} C_{\ell\ell}\, \delta_n \tag{152b}$$

where $\delta_n = \begin{cases} 1 & n=0 \\ 0 & n\neq 0 \end{cases}$

This particular type of real and imaginary parts of the coefficients of the Fourier series are due to the circular symmetry of the pattern around the axis of the array.

Let us take now two measurements of $|F(\phi)|^2$. The two measurements will differ from each other since, after the first measurement, we shall change the phase of the feed of a reference radiator is $A_o + iB_o$ by 180^o. There must be no interaction between the reference radiator and any other radiator. We take:

$$|F_1(\phi)|^2 \qquad f_{n_1} = f_{n_1}^R + if_{n_1}^1 \qquad A_o^{(1)} = 1 \quad B_o^{(1)} = 0 \tag{153a}$$

$$|F_2(\phi)|^2 \qquad f_{n_2} = f_{n_2}^R + if_{n_2}^i \qquad A_o^{(2)} = -1 \quad B_o^{(2)} = 0 \tag{153b}$$

where all the other amplitudes will be found with respect to the reference radiator. For n = odd (151b) may be rewritten as:

$$f_n^i = 2 \sum_{\ell=1}^{L} D_{\ell o} J_n(kx_{\ell o}) + 2 \sum_{\ell > m > o}^{L} \sum_{m>o}^{L} D_{\ell m} J_n(kx_{\ell m}) \tag{154a}$$

and for n = even (152b) may be rewritten as:

$$f_n^R = 2 \sum_{\ell=1}^{L} C_{\ell o} J_n(kx_{\ell o}) + 2 \sum_{\ell > m > o}^{L} \sum_{m>o}^{L} C_{\ell m} J_n(kx_{\ell m}) + \sum_{\ell=0}^{L} C_{\ell \ell} \delta_n \tag{154b}$$

Rewriting (154) twice for the two measurements in (153) and substracting one from the other we get:

n = odd

$$f_{n_1}^i - f_{n_2}^i = 2 \sum_{\ell=1}^{L} \left[D_{\ell o}^{(1)} - D_{\ell o}^{(2)} \right] J_n(kx_{\ell o}) \tag{155a}$$

n = even

$$f_{n_1}^R - f_{n_2}^R = 2 \sum_{\ell=1}^{L} \left[C_{\ell o}^{(1)} - C_{\ell o}^{(2)} \right] J_n(kx_{\ell o}) \tag{155b}$$

Using definitions (147) and substituting reference values (153) we get:

$$D_{\ell o}^{(1)} - D_{\ell o}^{(2)} = 2 B_\ell \tag{156a}$$

$$C_{\ell o}^{(1)} - C_{\ell o}^{(2)} = 2 A_\ell \tag{156b}$$

Substituting (156) in (155) we get:

n = odd

$$f_{n_1}^i - f_{n_2}^i = 4 \sum_{\ell=1}^{L} B_\ell J_n(kx_{\ell o}) \tag{157a}$$

n = even

$$f_{n_1}^{R} - f_{n_2}^{R} = 4 \sum_{\ell=1}^{L} A_\ell J_n (kx_{\ell o}) \tag{157b}$$

Let us define:

$$T_{12}(\phi) = |F_1(\phi)|^2 - |F_2(\phi)|^2 \tag{158a}$$

$$T_{12}(\phi) = \sum_{n=-\infty}^{+\infty} f_n^{12} e^{in\phi} \tag{158b}$$

$$f_n^{12} = f_{n_1} - f_{n_2} \tag{158c}$$

from definition (158) and by choosing the origin at the reference radiator $x_o = 0$ (157) becomes:

n = odd

$$\frac{1}{i} f_n^{12} = 4 \sum_{\ell=1}^{L} B_\ell J_n(kx_\ell) \tag{159a}$$

n = even

$$f_n^{12} = 4 \sum_{\ell=1}^{L} A_\ell J_n(kx_\ell) \tag{159b}$$

Since f_n^{12} is known by definition(158) and measurements, we have now stated in (159) the same problem as discussed in the beginning of this section with the formal solution given in (142b).

8. Conclusions

The suggestion is made for the use of arbitrarily distributed elements in linear arrays. A general theory has been given in order to analyze the performance of such arrays as well as to compare their overall performance.

In the arrays with equally spaced elements, we say that each element has one degree of freedom, i. e. its complex amplitude. A linear array with L equally spaced elements has L degrees of freedom, since we can match L coefficients of the Fourier series. By taking the general case of arrays with arbitrarily distributed elements, we add to each element another degree of freedom, i.e. its position along the axis of the array. Although there are certain restrictions on the position of the element along the axis of the array, the array with arbitrarily distributed elements has more degrees of freedom than a similar array with equally spaced elements. Therefore the array with arbitrarily distributed elements needs, in general, fewer elements in order to achieve the same performance as an array with equally spaced elements. In case we want to take the same number of elements, the performance of the array with arbitrarily distributed elements is better in general. In order to get more specific results we need a larger number of examples.

Using the above suggestions and methods of calculation , the designer of arrays will have more latitude in his work in order to achieve the required pattern and performance of the array. Although some of the calculations are rather cumbersome, more examples and more experience are necessary in order to simplify it. I hope that this work will help in better understanding the general theory of arrays, as well as in more economic design of arrays.

Appendix A

From equation (25) we get:

$$e^{iz_1\cos\theta} = 2\sum_{n=0}^{\infty}(\nu+n)i^n j_n^{\nu}(z_1)C_n^{\nu}(\cos\theta) \tag{A-1}$$

and the conjugate of it is:

$$e^{-iz_2\cos\theta} = 2\sum_{m=0}^{\infty}(\nu+m)(-i)^m j_m^{\nu}(z_2)C_m^{\nu}(\cos\theta) \tag{A-2}$$

multiplying the above we get:

$$e^{i(z_1-z_2)\cos\theta} = 4\sum_{m=0}^{\infty}\sum_{n=0}^{\infty}(\nu+m)(\nu+n)i^n(-i)^m \cdot$$

$$\cdot j_n^{\nu}(z_1)\, j_m^{\nu}(z_2)C_m^{\nu}(\cos\theta)C_n^{\nu}(\cos\theta) \tag{A-3}$$

Using the orthogonality in (26) we get:

$$\int_0^{\pi} e^{i(z_1-z_2)\cos\theta}\sin^{2\nu}\theta d\theta =$$

$$= \frac{\pi}{2^{2\nu-3}\Gamma^2(\nu)}\sum_{n=0}^{\infty}\frac{\Gamma(2\nu+n)}{n!}(\nu+n)j_n^{\nu}(z_1)j_n^{\nu}(z_2) \tag{A-4}$$

If we substitute $z_1 = z_2 = z$ in (A-4) we get: (A-5)

$$\sum_{n=0}^{\infty}\frac{\Gamma(2\nu+n)}{n!}(\nu+n)\left[j_n^{\nu}(z)\right]^2 = \frac{2^{2\nu-3}\Gamma^2(\nu)}{\pi}\int_0^{\pi}\sin^{2\nu}\theta d\theta$$

Case I: $\nu = 1/2$. The integral in (A-4) becomes:

$$\int_0^{\pi} e^{i(z_1-z_2)\cos\theta}\sin\theta d\theta = \int_{-1}^{+1} e^{i(z_1 - z_2)y}dy =$$

$$= \frac{e^{i(z_1-z_2)y}}{i(z_1-z_2)}\Bigg|_{-1}^{+1} = 2\,\frac{\sin(z_1-z_2)}{z_1-z_2} \tag{A-6}$$

From (A-4) and (A-6) for $\nu = \frac{1}{2}$ we get, using the identity in (24):

$$\sum_{n=0}^{\infty} (2n+1) j_n(z_1) j_n(z_2) = \frac{\sin(z_1 - z_2)}{z_1 - z_2} \tag{A-7}$$

Substituting in (A-7) $z_1 = z_2 = z$ we get:

$$\sum_{n=0}^{\infty} (2n+1) j_n^{\,2}(z) = 1 \tag{A-8}$$

Substituting in (A-7) $z_1 = -z_2 = z$ we get:

$$\sum_{n=0}^{\infty} (-)^n (2n+1) j_n^{\,2}(z) = \frac{\sin 2z}{2z} \tag{A-9}$$

(A-8) and (A-9) were given by Watson[8].

If we substitute in (A-7) $z_1 = \pi\ell$; $z_2 = \pi m$, where ℓ, m are integers, we get:

$$\sum_{n=0}^{\infty} (2n+1) j_n(\pi\ell) j_n(\pi m) = \delta_{\ell,m} = \begin{cases} 1 & \ell = m \\ 0 & \ell \neq m \end{cases} \tag{A-10}$$

Case II: For $\nu = \frac{3}{2}$ we get from (A-5):

$$\sum_{n=0}^{\infty} (n+1)(n+2)(2n+3) \left[j_n^{3/2}(z) \right]^2 = \frac{2}{3} \tag{A-11}$$

(A-11) corresponds to (A-8) in Case I. Other identities corresponding to Case I may be found easily enough, by using the general identity in (A-4).

Appendix B

Kapteyn[8] derived the following relation in Bessel functions:

$$\int_0^\infty J_\mu(z)\, J_\nu(z)\, \frac{dz}{z} = \frac{2}{\pi}\, \frac{\sin(\mu-\nu)\,\frac{\pi}{2}}{\mu^2-\nu^2} \tag{B-1}$$

where μ and ν are general real positive numbers.

If we take μ and ν to be integers, (B-1) has the orthogonality properties only if the difference $\mu-\nu$ is an even integer. In order to get orthogonality properties for all integer orders n, let us consider another integral:

$$I_{n,m} = \int_{-\infty}^{+\infty} J_n(z)\, J_m(z)\, \frac{dz}{|z|} \tag{B-2}$$

From the general identity:

$$J_n(-z) = (-)^n\, J_n(z) \tag{B-3}$$

we see that Bessel functions with odd orders are odd and with even orders are even. When n,m are both odd or both even, the difference (n-m) is even and the orthogonality properties of (B-1) hold. When n is odd and m is even or vice versa, the integrand in (B-2) is an odd function and will be integrated to zero.

Therefore (B-2) has general orthogonality properties for integer orders of Bessel function, and using (B-1) it may be rewritten as:

$$\int_{-\infty}^{+\infty} J_n(z)\, J_m(z)\, \frac{dz}{|z|} = \frac{1}{n}\, \delta_{m,n} = \begin{cases} \frac{1}{n} & n=m\neq 0 \\ 0 & n\neq m \end{cases} \tag{B-4}$$

Using (B-1) we can derive orthogonality properties for spherical Bessel functions defined[9] as:

$$j_n(z) = \sqrt{\frac{\pi}{2z}}\, J_{n+1/2}(z) \tag{B-5}$$

From the power series for $j_n(z)$ we can see that:

$$j_n(-z) = (-)^n j_n(z) \tag{B-6}$$

Substituting in (B-1)

$$\mu = n+1/2 \qquad \nu = m+1/2 \tag{B-7}$$

and using definition in (B-5) we get:

$$\int_0^{\infty} j_n(z)\, j_m(z)\, dz = \frac{\sin (n-m)\frac{\pi}{2}}{(n+1/2)^2-(m+1/2)^2} \tag{B-8}$$

Using (B-6) and the same arguments as above, we can find from (B-8) the orthogonality property:

$$\int_{-\infty}^{+\infty} j_n(z)\, j_m(z)\, dz = \frac{\pi}{2n+1}\, \delta_{m,n} \tag{B-9}$$

where n,m are positive integers.

For the particular case n=m=0 we know that:

$$j_0(z) = \frac{\sin z}{z} \tag{B-10}$$

and substituting in (B-9) we get:

$$\int_{-\infty}^{+\infty} \frac{\sin^2 z}{z^2}\, dz = \pi \tag{B-11}$$

(B-11) may be also found elsewhere[11].

Appendix C

Let us find a direct relation between a continuous line current distribution and its far zone pattern.

From (4a) we can find the far zone pattern of a continuous line current source of length 2ℓ to be:

$$F(\phi) = \int_{-\ell}^{+\ell} A(x)\, e^{ikx\sin\phi}\, dx \tag{C-1}$$

substituting $y=kx$ and $A(y)=\frac{1}{k}A(x)$ we get:

$$F(\phi) = \int_{-k\ell}^{+k\ell} A(y)\, e^{iy\sin\phi} dy \tag{C-2}$$

Expanding the far zone pattern in a Fourier series:

$$F(\phi) = \sum_{n=-\infty}^{+\infty} f_n\, e^{in\phi} \quad . \tag{C-3}$$

and using the expansion (5a) in (C-2) we get:

$$f_n = \int_{-k\ell}^{+k\ell} A(y)\ \ J_n(y)\, dy \tag{C-4}$$

Let us assume that the current distribution along the line current 2ℓ is in the form of a series:

$$A(y) = a_o\, \delta(y) + \sum_{m=1}^{\infty} a_m\ \frac{J_m(y)}{|y|} \tag{C-5}$$

where $\delta(y)$ is the Dirac delta function and represents a dipole at the origin. Substituting (C-5) in (C-4) we get:

$$f_n = a_o \int_{-k\ell}^{+k\ell} \delta(y)\ \ J_n(y)dy + \sum_{m=1}^{\infty} a_m \int_{-k\ell}^{+k\ell} J_n(y)\ J_m(y)\frac{dy}{|y|} \tag{C-6}$$

By the definition of Dirac delta function:

$$\int_{-k\ell}^{+k\ell} \delta(y)\, J_n(y)\, dy = J_n(0) \tag{C-7}$$

Taking the line current so that $\ell \to \infty$ and using the orthogonality properties in (B-4), (C-6) becomes:

$$f_n = a_o J_n(0) + \sum_{m=1}^{\infty} a_m \frac{1}{n} \delta_{m,n} \tag{C-8}$$

by taking different n in (C-8) we get:

$$f_o = a_o \qquad f_n = \frac{1}{n} a_n \tag{C-9}$$

(C-9) gives a direct relation between current distribution (C-5) and pattern (C-3).

Similarly (C-2) may be given as:

$$F(\theta) = \int_{-k\ell}^{+k\ell} A(y)\, e^{iy\cos\theta}\, dy \tag{C-10}$$

Expanding the pattern in Legendre polynomials:

$$F(\theta) = \sum_{n=0}^{\infty} (2n+1)\, d_n P_n(\cos\theta) \tag{C-11}$$

and using expansion (15) in (C-10), comparing with (C-11) we get:

$$i^{-n} d_n = \int_{-k\ell}^{+k\ell} A(y)\, j_n(y)\, dy \tag{C-12}$$

assuming for the current distribution the series:

$$A(y) = \sum_{m=0}^{\infty} a_m j_m(y) \tag{C-13}$$

and substituting in (C-12) we get:

$$i^{-n} d_n = \sum_{m=0}^{\infty} a_m \int_{-k\ell}^{+k\ell} j_m(y)\, j_n(y)\, dy \tag{C-14}$$

taking the length of the line current $\ell \to \infty$ and using the orthogonality property (B-9), we can get from (C-14):

$$i^{-n} d_n = \sum_{m=0}^{\infty} a_m \frac{\pi}{2n+1} \delta_{m,n} \tag{C-15}$$

(C-15) may be expressed using the definition of $\delta_{m,n} = \begin{cases} 1 & m=n \\ 0 & m \neq n \end{cases}$ as:

$$(2n+1)\, d_n = \pi\, i^n a_n \tag{C-16}$$

From (C-11), (C-13) and (C-16) we see that for every set of coefficients a_n we have corresponding line current and a pattern as follows:

$$A(y) = \sum_{n=0}^{\infty} a_n j_n(y) \tag{C-17a}$$

$$\frac{1}{\pi} F(\theta) = \sum_{n=0}^{\infty} i^n a_n P_n(\cos\theta) \tag{C-17b}$$

It must be noted that (C-17a) has a finite current distribution along the line, while (C-5) has a dipole with infinite current at the origin; it produces the dipole field f_o in (C-3) as may be seen in (2).

The same far zone pattern may be produced by infinite number of different current distributions since the problem is not unique. Other solutions besides the above two might as well exist.

In case we want the current (C-5) to give a predominate effect by a shorter line current, we might differentiate (C-2) p times with respect to $\sin\phi$ and get:

$$\frac{1}{i^p} \frac{d^p F(\phi)}{d(\sin\phi)^p} = \int_{-k\ell}^{+k\ell} A(y)\, y^p\, e^{iy\sin\phi}\, dy \tag{C-18}$$

(C-18) has the same form as (C-2) if we take:

$$F^{(p)}(\phi) = \frac{1}{i^p} \frac{d^p F(\phi)}{d(\sin\phi)^p} \quad ; \quad A^{(p)}(y) = y^p A(y) \tag{C-19}$$

and we can comtinue with the "new" current and pattern as before.

REFERENCES

1. Wolff, I. "Determination of the Radiating System Which Will Produce a Specified Directive Characteristic", Proc. I.R.E., 25 May , 1937

2. Schelkunoff, S.A., "A Mathematical Theory of Linear Arrays" Bell System Technical Journal, January 22, 1943.

3. Dolph, C.L., "A Current Distribution for Broadside Arrays which Optimizes the Relationship Between Beamwidth and Side Lobe Level", Proc. I.R.I 34, June 1946.

4. Woodward, P.M., and Lawson, J.D., "The Theoretical Precision with which Arbitrary Radiation Pattern may be Obtained from a Source of Finite Size". Proc. I.E.E, 95, Sept. 1948.

5. Chu, L. J., "Physical Limitations of Omni-Directional Antennas" J.A.P. 19, Dec. 1948.

6. Arsac, J., "Etude theorique des reseaux d'antennes en radiastronomie et realisation de l'un d'eux" Thesis (French) Faculty of Science, Univ. of Paris, 1955.

7. Silver, S., Microwave Antenna Theory and Design, McGraw Hill, 1949

8. Watson, G.N., A Treatise on the Theory of Bessel Functions, Cambridge, 1952

9. Stratton, J.A., Electromagnetic Theory, McGraw Hill, 1941

10. Magnus, W., and Oberhettinger, F., Formulas and Theorems for the Functions of Mathematical Physics Chelsea Pub. Co., New York 1954.

11. Dwight, H.B., Tables of Integrals and Other Mathematical Data. McMillan Co. 1947.

Chief of Naval Research
Navy Department
Washington 25, D.C.
2 Attn: Code 427
1 460

Director
Naval Research Laboratory
Technical Information Officer
Washington 25, D.C.
6 Attn: Code 2000
1 2020

Commanding Officer
Office of Naval Research, Br.Office
1030 E. Green Street
1 Pasadena 1, California

Commanding Officer
Office of Naval Research, Br.Office
1000 Geary Street
1 San Francisco 9, California

Commanding Officer
Office of Naval Research, Br.Office
The John Crerar Library Building
86 East Randolph Street
1 Chicago 1, Illinois

Commanding Officer
Office of Naval Research,Br.Office
346 Broadway
1 New York 13, New York

Commanding Officer
Office of Naval Research, Br. Office
Navy # 100, Fleet Post Office
1 New York, New York

Chief, Bureau of Ordnance
Navy Department
Washington 25, D. C.
1 Attn: Code Rad

Chief, Bureau of Ships
Navy Department
Washington 25, D.C.
2 Attn: Code 838

Chief, Bureau of Aeronautics
Navy Department
Washington 25, D.C.
1 Attn: Code RE-51

Chief of Naval Operations
Navy Department
Washington 25, D.C.
1 Attn: OP 371
OP 30
OP 92

Director
Naval Ordnance Laboratory
1 White Oak, Maryland

Commander
Naval Electronics Laboratory
1 San Diego, California

U.S. Naval Air Missile Test Center
1 Point Mugu, California

Commander Naval Air Development
Center
Johnsville, Pennsylvania
1 Attn: Code ADL

U.S. Naval Post Graduate School
Monterey, California
1 Attn: Librarian

U.S. Coast Guard
1300 E. Street N.W.,
Washington 25, D.C.
1 Attn: EES

Assistant Secretary of Defense
(Research and Development)
Research and Development Board
Department of Defense
1 Washington 25, D.C.

Office of the Chief Signal Officer
Pentagon
Washington 25, D.C.,
1 Attn: SIGRT

Signal Corps Engineering Laboratories
Fort Monmouth, New Jersey
1 Attn: Mr. G. H. Woodward

Armed Services Technical Information
Agency, Document Service Center
Knott Building
5 Dayton 2, Ohio

H. A. Brunswick, Chief
Systems Component Branch
Electronic Warfare Division
White Sands Signal Corps Agency
1 White Sands Proving Ground, N.M.

Commanding Officer
Signal Signal Laboratory
Fort Monmouth, New Jersey
1 Attn: Mr. Vincent J. Rublin

Director
Ballistic Research Laboratories
Aberdeen Proving Ground
Maryland
1 Attn: Ballistic Measurements
Laboratory

Commanding General
Signal Corps Engineering Laboratories
Evans Signal Laboratory Area
Building #7, Belmar, New Jersey
1 Attn: Technical Documents Center

Watson Laboratories
Library, AMC
Red Bank, New Jersey
1 Attn: ERASMI

Commanding General
Air Force Cambridge Research Center
230 Albany Street
Cambridge 39, Massachusetts
1 Attn: CRRE

Commanding General
Air Research and Development Command
P.O. Box 1395
Baltimore 3, Maryland
1 Attn: RDTDR
1 RDTDRR
RDTDRM

Commanding General
Wright Air Development Center
Wright-Patterson Air Force Base
Ohio
1 Attn: WCRRO-2
1 WCLRC

Commanding General
Rome Air Development Center
Griffiss Air Force Base
Rome, New York
1 Attn: RCRW

Commander
Air Force Cambridge Research Center
Air Research and Development Command
Laurence G. Hanscom Field
Bedford, Massachusetts
Attn: CRRDO

1 Office of Technical Services
Department of Commerce
Washington 25, D. C.

Library,
Boulder Laboratories
National Bureau of Standards
Boulder, Colorado
2 Attn: Mrs. V. S. Harver,
Librarian

Department of Electrical Engineering
Cornell University
Ithaca, New York
1 Attn: Dr. H. G. Booker

Electrical Engineering Research
Laboratory
University of Illinois
Urbana, Illinois
1 Attn: Dr. R. K. Dubmel

Research Laboratory of Electronics
Document Room
Massachusetts Institute of Technology
Cambridge 39, Massachusetts
1 Attn: Mr. J. Hamlet

The Johns Hopkins University
Radiation Laboratory
1315 St. Paul Street
Baltimore 2, Maryland
1 Attn: - Mr. H. H. Ling

Technical University
Department of Electrical Engineering
Delft, Holland
Via CRE London
1 Attn: - Prof. J. P. Sheehan

Electrical Engineering Department
University of Texas
Box F, University Station
1 Austin, Texas

Electronics Research Laboratory
Stanford University
Stanford, California
1 Attn: Dr. F. E. Terman

Mathematics Research Group
New York University
45 Astor Place
New York, New York
1 Attn: Dr. M. Kline

Craft Laboratory
Harvard University
303A Pierce Hall
Cambridge 38, Massachusetts
1 Attn: Technical Reports Collection

Antenna Laboratory
Ohio State University
Research Foundation
Columbus, Ohio
1 Attn: Dr. Tai

Brooklyn Polytechnic Institute
Microwave Research Institute
55 Johnson Street
Brooklyn 1, New York
1 Attn: Dr. A. Oliver

Electronics Division
Denver Research Institute
University of Denver
Denver 10, Colorado
1 Attn: Mr. Carl A. Hedberg, Head

Illinois Institute of Technology
Technology Center
1 Chicago 16, Illinois -

University of Florida
Board of Control
1 Gainesville, Florida -

Regents of the University of
Michigan
1 Ann Arbor, Michigan -

Willow Run Research Center
University of Michigan
Ypsilanti, Michigan
1 Attn: - Dr. K. Siegel

Columbia University Radiation Labs.,
New York 27, New York
1 Attn: - Prof. W. E. Lamb, Jr.

University of Pennsylvania
Randall Morgan Laboratory of Physics
1 Philadelphia 4, Pennsylvania -

California Institute of Technology
Pasadena, California
1 Attn: - C. H. Papas

Georgia Institute of Technology
Atlanta, Georgia
1 Attn: - Mrs. J. Pauley Crossland

Yale University
Department of Electrical Engineering
1 New Haven, Connecticut -

Cavendish Laboratory
Cambridge University
Radiophysics Division
Cambridge, England
Via, CRE London
1 Attn: - Mr. J. A. Ratcliffe

Laboratory for Telephony and
Telegraphy
Royal Technical University
Gamvoldsgade 10, Copenhagen
Denmark
Via, CRE London
1 Attn: - Prof. N. L. Knudsen

Stanford Research Institute
Stanford, California
1 Attn: Dr. John V. N. Granger

Hughes Research Laboratory
Hughes Aircraft Co.
Culver City, California
1 Attn: - Head, Antenna Research
Microwave Laboratory

Hughes Aircraft Company
Research and Development Library
Culver City, California
1 Attn: - John T. Milek

RCA Laboratories
Princeton, New Jersey
1 Attn: - E. W. Herold
Harwell Johnson

Varian Associates
611 Hansen way
Palo Alto, California
1 Attn: - Technical Library

Mr. R. C. Crowding, Librarian
Bell Telephone Laboratories, Inc.
463 west Street
1 New York 14, New York

Boeing Aircraft Company
Physical Research Unit
Seattle 14, Washington
1 Attn: - Mr. R. W. Illman

The Rand Corporation
1700 Main Street
Santa Monica, California
1 Attn: - Margaret Anderson,
Librarian

General Telecommunication
600 Washington Avenue
Carlstadt, New Jersey
1 Attn: - W. Derrick, Contract Section

British Broadcasting Corporation
Research Laboratory
Kingswood Warren
Tadworth, Surrey, England
1 Attn: - W. Procter Wilson
Harold Page

Dr. C. J. Bouwkamp
Philips Research Laboratories
N.V. Philip's Gloeilampenfabrieken
Eindhoven, Netherlands -
1 Via, CRE London

Airpath Research Associates
3130 Fourth Avenue
1 San Diego 3, California

Douglas Aircraft Company, Inc.
El Segundo Division
1 El Segundo, California

UNCLASSIFIED